Optimization Algorithms for Integration of Design, Control, and Scheduling for Chemical Processes Subject to Disturbances and Uncertainty

by

Robert Koller

A thesis
presented to the University of Waterloo
in fulfillment of the
thesis requirement for the degree of
Master of Applied Science
in
Chemical Engineering

Waterloo, Ontario, Canada, 2017

Author's Declaration

I hereby declare that I am the sole author of this thesis. This is a true copy of the thesis, including any required final revisions, as accepted by my examiners.

I understand that my thesis may be made electronically available to the public.

Abstract

Optimization of multiproduct processes is vital for process performance, especially during dynamic transitions between operating points. However, determining the optimal operating conditions can be a challenging problem, since many aspects must be considered, such as design, control, and scheduling. This problem is further complicated by process disturbances and parameter uncertainty, which are typically randomly distributed variables that traditional methods of optimization are not equipped to handle. Multi-scenario approaches that consider every possible realization are also impractical, as they quickly become computationally prohibitive for large-scale applications. Therefore, new methods are emerging for generating robust solutions without adding excessive complexity. This thesis focuses on the development of two optimization methods for the integration of design, control, and scheduling for multi-product processes in the presence of disturbances and parameter uncertainty.

Firstly, a critical set method is presented, which decomposes the overall problem into flexibility and feasibility analyses. The flexibility problem is solved under a critical (worst-case) set of disturbance and uncertainty realizations, which is faster than considering the entire (non-critical) set. The feasibility problem evaluates the dynamic feasibility of the entire set, and updates the critical set accordingly, adding any realizations that are found to be infeasible. The algorithm terminates when a robust solution is found, which is feasible under all identified scenarios. To account for the importance of grade transitions in multiproduct processes, the proposed framework integrates scheduling into the dynamic model by the use of flexible finite elements. The critical set method is applied to two case studies, a continuous stirred-tank reactor (CSTR) and a plug flow reactor (PFR), both subject to process disturbance and parameter uncertainty. The proposed method is shown to return robust solutions that are of higher quality than the traditional sequential method, which determines the design, control, and scheduling independently.

This work also considers the development of a back-off method for integration of design, control, and scheduling for multi-product systems subject to disturbances and parameter uncertainty. The key

feature of this method is the consideration of stochastic random variables for the process disturbance and parameter uncertainty, while most works discretize these variables. This method employs Monte Carlo (MC) sampling to generate a large number of random realizations, and simulate the system to determine feasibility. Back-off terms are determined and incorporated into a new flexibility analysis to approximate the effect of stochastic uncertainty and disturbances. The back-off terms are refined through successive iterations, and the algorithm converges, terminating on a solution that is robust to a specified level of process variability. The back-off method is applied to a similar CSTR case study for which optimal design, control, and scheduling decisions are identified, subject to stochastic uncertainty and disturbance. Another scenario is analyzed, where the CSTR is controlled in open-loop, and the control actions are determined directly from the optimization. The back-off method successfully produces solutions in both scenarios, which are robust to specified levels of variability, and consider stochastic representations of process disturbance and parameter uncertainty.

The results from the case studies indicate that there are interactions between optimal design, control, scheduling, disturbance, and uncertainty, thus motivating the need for integration of all these aspects using the methods described in this thesis. The solutions provided by the critical set method and the back-off can be compared, since the methods are applied to the same CSTR case study, aside from the differences in disturbance and uncertainty. The back-off method offers a slightly improved solution, though the critical set method demands much less computational time. Therefore, both methods have benefits and limitations, so the optimal method would depend on the available computational time, and the desired quality and robustness of the solution.

Acknowledgements

Firstly, I would like to express many thanks to my supervisor Professor Luis Ricardez-Sandoval for his guidance and support during my entire Master's program. I would also like to extend my thanks to the readers of my thesis, Professor Hector Budman and Professor Peter Douglas.

I would like to thank my group members Mina Rafiei, M. Hossein Sahraei, Zhenrong He, and Manuel Tejeda for their continued assistance and companionship throughout my research studies.

Finally, I would like express my deepest gratitude to my fiancée who has always been there for me.

Table of Contents

List of Figures

List of Tables

List of Abbreviations

CNS	Constrained Nonlinear System
CSTR	Continuous Stirred-Tank Reactor
GAMS	General Algebraic Modelling System (software)
IP	Integer Programming
KKT	Karush-Kuhn-Tucker
MC	Monte Carlo
MIDO	Mixed-Integer Dynamic Optimization
MINLP	Mixed-Integer Nonlinear Programming
MPC	Model Predictive Control
NLP	Nonlinear Programming
ODE	Ordinary Differential Equation
PDE	Partial Differential Equation
PFR	Plug Flow Reactor
PI	Proportional and Integral (control)
PSE	Power Series Expansion

List of Symbols

a	Index for inequality constraints $\boldsymbol{g}$
$\boldsymbol{\mathcal{A}}$	Matrix of orthogonal collocation weights
$\boldsymbol{b}(t)$	Back-off terms at time t
$b_{i,j,k}$	Back-off terms in region i, finite element j, and collocation point k
$\boldsymbol{c}$	Critical set of realizations
$\boldsymbol{\mathcal{C}}$	Control decisions
$\boldsymbol{d}(t)$	Vector of process disturbances
$\bar{\boldsymbol{d}}(t)$	Nominal value for vector of process disturbances
$\boldsymbol{d}_{ijk}^{\omega}$	Vector of process disturbances at discrete state ω, in region i, finite element j, and collocation point k, corresponding to realization ω of process disturbance
$\boldsymbol{\mathcal{D}}$	Design decisions
$E[z]_n$	Expected total process cost in iteration n of the back-off algorithm
$\boldsymbol{\mathcal{E}}$	Vector of decision variables $\boldsymbol{\mathcal{E}} = \{\boldsymbol{\mathcal{D}}, \boldsymbol{\mathcal{C}}, \boldsymbol{\mathcal{S}}, \boldsymbol{\Delta t}\}$
$\boldsymbol{f}$	Vector of differential equations
$\boldsymbol{g}$	Vector of inequality constraints
G	Number of product grades to be produced
$\boldsymbol{h}$	Vector of equality constraints
i	Index for time regions
I	Number of time regions
j	Index for finite elements
J	Number of finite elements per time region
k	Index for collocation points
K	Number of collocation points per finite element

m	Index for Monte Carlo simulations
M	Number of Monte Carlo simulations in each iteration of the back-off algorithm
n	Algorithm iteration number
$\boldsymbol{p}$	Vector of uncertain parameters
$\bar{\boldsymbol{p}}$	Nominal value for vector of uncertain parameters
$\boldsymbol{p}^{\theta}$	Vector of uncertain parameters corresponding to realization θ of parameter uncertainty
$\boldsymbol{S}$	Scheduling sequence decisions
t	Time
t_{end}	Total duration of production horizon
$\boldsymbol{\Delta t}$	Region duration decisions (for all i)
Δt_i	Total duration of time region i
δt_i	Duration of one finite element in time region i
$\boldsymbol{u}(t)$	Vector of process inputs
$\boldsymbol{u}_{ijk}^{\theta,\omega}$	Vector of process inputs in region i, finite element j, and collocation point k, corresponding to realization (θ, ω) of process disturbance and parameter uncertainty
$\boldsymbol{x}(t)$	Vector of process states
$\dot{\boldsymbol{x}}(t)$	Vector of process state derivatives
$\boldsymbol{x}_{ijk}^{\theta,\omega}$	Vector of process states in region i, finite element j, and collocation point k, corresponding to realization (θ, ω) of process disturbance and parameter uncertainty
$\boldsymbol{y}(t)$	Vector of process outputs
$\boldsymbol{y}^{\boldsymbol{sp}}(t)$	Vector of process output set-points
$\boldsymbol{y}_{ijk}^{\theta,\omega}$	Vector of process outputs in region i, finite element j, and collocation point k, corresponding to realization (θ, ω) of process disturbance and parameter uncertainty

$(\boldsymbol{y}^{sp})_{ijk}$ Vector of process outputs in region i, finite element j, and collocation point k, corresponding to realization (θ, ω) of process disturbance and parameter uncertainty

$Y_{a,ijk}^{\theta,\omega}$ Binary variables to indicate if worst case variability occurs for constraint g_a in region i, finite element j, and collocation point k, corresponding to realization (θ, ω) of process disturbance and parameter uncertainty

$\mathbf{Y^{sp}}$ List of process set-points, unordered

z Total process cost

$\alpha_{a,ijk}^{\theta,\omega}$ Slack variables for constraint g_a in region i, finite element j, and collocation point k, corresponding to realization (θ, ω) of process disturbance and parameter uncertainty

$\boldsymbol{\beta}$ List of process set-points, in order of production

Γ Maximum expected constraint violation predicted by Monte Carlo simulations

$\zeta^{\theta,\omega}$ Weight for realization (θ, ω) in critical set approach

θ Index for realizations of process disturbance $\boldsymbol{d}$

Θ Number of realizations for process disturbance $\boldsymbol{d}$

λ Back-off multiplier

$\mu_{m,i,j,k}$ Estimated mean constraint value at region i, finite element j, and collocation point k, after m Monte Carlo simulations

$\sigma_{m,i,j,k}^2$ Estimated constraint variance at region i, finite element j, and collocation point k, after m Monte Carlo simulations

Φ_n Maximum infeasibility in iteration n of the critical set algorithm

$\boldsymbol{\psi}$ Function to determine process set-points from scheduling decisions

ω Index for realizations of uncertain parameters $\boldsymbol{p}$

Ω Number of realizations for uncertain parameters $\boldsymbol{p}$

Chapter 1: Introduction

Multiproduct processes are widely used in different sectors due to their versatility and convenience, e.g. oil & gas (Harjunkoski et al., 2009), pharmaceutical (Nie and Biegler, 2012), and polymer production (Harjunkoski et al., 2009; Terrazas-Moreno et al., 2008). To remain competitive, companies are required to operate their systems at nearby optimal conditions that can efficiently produce their products under environmental, safety and product specification constraints. Most major chemical companies have invested in large computing networks that are dedicated to solving large-scale process optimization problems (Seferlis and Georgiadis, 2004). Finding optimal operating conditions can be very challenging, especially for large systems, where there are many aspects that can influence the process economics, such as design, control, and scheduling. The sequential method offers the simplest approach, where each aspect is optimized separately, in small independent problems. Though this method is fast, it relies on a large amount of assumptions, which can heavily influence the final solution, rendering it suboptimal or infeasible. Despite those limitations, the sequential method is widely used in industry to its superior speed and ease of implementation. Theoretically, the integrated method is a better approach, where the design, control, and scheduling are solved simultaneously in one large optimization problem. This method accounts for all the interactions between the aspects, but the high computational complexity limits the practical applications of this method. Decomposition algorithms have been proposed to break the integrated method into two sub-problems, with the goal of reducing problem complexity while maintaining the same solution quality. Such algorithms have been widely researched for integration of design and control, but the addition of scheduling has only been considered by a few publications.

Furthermore, uncertainty and process disturbances can have a significant effect on process optimality and feasibility, as model parameters and external perturbations are typically not known *a priori* with absolute certainty, resulting in variability in process output. For a process that is optimized only at nominal conditions, i.e. uncertain parameters and disturbances set to their nominal (expected) values, the solution can become suboptimal or infeasible when it is subjected to parameter uncertainty and process

disturbance, as operating limits are surpassed. Therefore, it is necessary to find robust solutions that can accommodate a specified level of uncertainty. Robust solutions are typically more conservative than nominal solutions, but the advantage is that they can accommodate uncertainty. A very basic method of producing robust solutions is the use of overdesign factors, where a decision variable is altered from its optimal point, to reduce the effect of uncertainty. This method does not guarantee an optimal result under uncertainty, but it is usually sufficient, and simple to implement, leading to its widespread use in industry for accommodating uncertainty (Brengel and Seider, 1992). More advanced methods are emerging with the potential to provide higher quality solutions at the cost of higher computational complexity (Ricardez Sandoval et al., 2008). The multi-scenario method and the back-off method will be described in the literature review.

1.1 Research Objectives

The objective of this study is to develop optimization methods for integration of design, control, and short-term scheduling, subject to disturbance and uncertainty. The novelty of this work is that it considers the non-linear dynamic process model, along with disturbances and parameter uncertainty, whereas most previous works on integrated optimization have disregarded one or more of those aspects. The scheduling sequence and transition times are explicitly accounted for in the dynamic model by the use of orthogonal collocation on finite elements, where a flexible implementation allows the finite elements to vary in size.

This thesis will investigate two different methods for optimization under uncertainty: the critical set method and the back-off method. The critical set method consists of an iterative algorithm that finds critical (worst-case) realizations of disturbance and uncertainty, and optimizes with respect to the "critical set" so that all realizations can be accommodated by the solution. The back-off method also employs an iterative approach, using Monte Carlo (MC) sampling to simulate the system and generate back-off terms.

These back-off terms and incorporated into the optimization to approximate the effect of stochastic uncertainty and disturbances. Both of the methods in this thesis have the potential to provide higher quality solutions than traditional methods. The methods will be tested on a multi-product continuous stirred tank reactor (CSTR) and a plug flow reactor (PFR). In each of these case studies, the optimal design, control, and scheduling decisions are identified, subject to uncertainty and disturbance.

The methods are applied to two case studies: a non-isothermal CSTR, and an isothermal PFR. The solutions are compared to the sequential method, which determines the optimal design, control, and scheduling one at a time, ignoring interactions. The solutions are compared in terms of solution quality and computational complexity, to demonstrate the merit of the methods presented in this thesis, and expand upon research in the area of integrated process optimization.

1.2 Structure of Thesis

This thesis is organized into chapters as follows:

Chapter 2 provides a detailed literature review, outlining the variety of methods that have been used for integration of design, control, and/or scheduling. Methods for dealing with uncertainty, such as the back-off method, are also presented. Relevant contributions are discussed in detail, to highlight the expansions made in the present work.

Chapter 3 presents the critical set method. The overall problem is defined, and the conceptual optimization is shown. The time discretization is explained, and the approximations for uncertainty and disturbance are presented. The critical set method is explained using an algorithm flowchart and a formal mathematical representation. This method is applied to two case studies, a CSTR system and a PFR system, and the results are analyzed. The content in this chapter has been published in Computers & Chemical Engineering (Koller and Ricardez-Sandoval, 2017a), and in the conference proceedings of the 27th European Symposium on Computer-Aided Process Engineering (Koller and Ricardez-Sandoval,

2017b). Those papers were written entirely by myself, and were edited by my supervisor, Luis Ricardez-Sandoval. Permission has been granted from the publisher to use the published content in this thesis.

Chapter 4 presents the back-off method. The problem definition and time discretization are the same as with the previous method, and the differences in uncertainty and disturbance definitions are described. This method is also explained using an algorithm flowchart and a formal mathematical representation. The back-off method is applied to the CSTR case study, considering two different controller configurations, and the results are analyzed. A standard PI controller is tested, as well as a dynamic controller, which determines the control actions directly from the optimization. The content in this chapter has been submitted to the American Institute of Chemical Engineers (AIChE) Journal. That paper was written entirely by myself, and was edited by my supervisor, Luis Ricardez-Sandoval, and a collaborator, Lorenz T. Biegler at Carnegie Mellon University.

Chapter 5 summarizes the methods and results of this thesis, and presents the conclusions. Based on the limitations of the proposed methods, recommendations are provided for future work in the area of integration of design, control, and scheduling.

Chapter 2: Literature Review

Determining the optimal design, control, and scheduling for a process can vary greatly in difficulty depending on the method used. The sequential method and the integrated method are two general methods that are explained in this section, and the contributions of relevant works are summarized. The effect of disturbance and uncertainty on process optimization is discussed, along with an outline of methods that can account for these unknown variables. The multi-scenario approach and the back-off approach can generate solutions that are robust to uncertainty, although they approach the problem very differently. The benefits and limitations of all these approaches are discussed in this section. The expected contribution of the work in this thesis is explained, as it fills a gap in the research area.

2.1 Integration of Design, Control, and Scheduling

The simplest approach to address optimal process design, scheduling and control for large process networks is the sequential approach, where the design, control, and scheduling of the system are all considered separately (Patil et al., 2015; Zhuge and Ierapetritou, 2012). This approach is popular in many industries (Mohideen et al., 1996) because solutions can be obtained very quickly, due to the independence of the sub-problems. Although the sequential method is practical and easy to implement, there are many limitations. Since each sub-problem is solved independently, the interactions between design, control, and scheduling are neglected, even though it has been recognized that these interactions can be significant (Flores-Tlacuahuac and Grossmann, 2011; Pistikopoulos and Diangelakis, 2015; Zhuge and Ierapetritou, 2012). Furthermore, assumptions need to be made in each sub-problem, e.g. steady-state operation or adding overdesign factors, and these assumptions may be invalid or return expensive plant designs. Hence, the solution generated by the sequential approach is likely to be suboptimal, and may become dynamically infeasible in some cases leading to the specification of invalid designs and

scheduling sequences (Chu and You, 2014a). These limitations have motivated the development of more reliable and robust methods of determining design, control, and scheduling.

The integrated approach is a more advanced method, in which the design, control, and scheduling are optimized simultaneously, for the purpose of considering interactions. This approach has the potential to provide attractive solutions, which are more optimal and reliable (Chu and You, 2014b; Mendez et al., 2006; Nie et al., 2015; Patil et al., 2015). However, optimization of large-scale and/or complex systems involving various factors can be challenging, particularly with multiproduct process units, where the process operation depends on many aspects, such as design (equipment sizing), control (controller structure and tuning), and scheduling (product sequencing and transitions). While several studies have considered integration of design and control (Ricardez-Sandoval et al., 2009; Sakizlis et al., 2004; Yuan et al., 2012), integration of scheduling with design and control decisions has not been deeply explored. In the case of multi-product plants, it can be advantageous to account for scheduling decisions at the design stage since it dictates the dynamic transitions between the different products to be produced, which in turn, depend on design and control (Bhatia and Biegler, 1996; Flores-Tlacuahuac and Grossmann, 2011; Pistikopoulos and Diangelakis, 2015). For large-scale problems, the integrated method has a high computational cost due to the large number of variables involved, including the binary variables considered in the scheduling formulation. To solve such large problems, assumptions would have to be made to reduce the problem size. Despite the growing interest in integrated optimization, there is no commercial software which is specifically designed to solve these types of problems (Pistikopoulos and Diangelakis, 2015). Methods that have been used for solving such problem are discussed in the next subsection, along with a discussion on process disturbances and parameter uncertainty.

As shown in Table 1, previous publications primarily focus on design and control, but publications are also available for integration of design and scheduling, or control and scheduling. Due to problem complexity, few publications address the integration of design, control, and scheduling. In one of the first studies, the design, control, and scheduling of a methyl-methacrylate process are optimized

simultaneously (Terrazas-Moreno et al., 2008). The scheduling decisions include production order and transition times, which account for process dynamics. That formulation included parameter uncertainty, as values that are selected from a discrete set; process disturbances were not considered. In lieu of a closed-loop control scheme, the profile of the manipulated variable was directly obtained from dynamic optimization. In another study (Patil et al., 2015), the integration was applied to multiproduct processes under disturbance and uncertainty. Decisions were made on equipment sizing, steady-state operating conditions, control tuning, production sequence, and transition times between product grades. The total cost was based on the worst-case disturbance frequency, which was identified using frequency response analysis on the linearized process model. One limitation is that the non-linear process model was linearized around the steady state operating conditions, which reduced the complexity of the problem, but introduced approximations to the model behavior and therefore to the resulting solution. A recent work presents a generalized software solution for integrated optimization problems, summarizes recent efforts in the subject area, and presents simultaneous design and operational optimization of heat and power cogeneration units (Pistikopoulos and Diangelakis, 2015).

The main drawbacks of previous publications are discussed in this paragraph. Many papers that consider scheduling in their formulation do not consider dynamic operation of the process (Chu and You, 2014b, 2014c; Zhuge and Ierapetritou, 2012). Instead, they assume a perfect controller, providing an ideal profile for the controlled variable. This allows the scheduling component to be solved independently, greatly simplifying the problem. In this thesis, the dynamic process model will be used to accurately simulate the process dynamics, which are especially relevant during scheduling transitions. Many publications linearize their process model, which simplifies the optimization problem, and allows the use of frequency analysis to determine a critical frequency for the process disturbance. This reduces the computational complexity, but the linearization introduces error into the solution, especially in highly non-linear cases. This thesis will use the full non-linear process model to maintain solution accuracy.

Table 1: Previous Works on Integration of Design, Control, and/or Scheduling

Topic	Authors	Contributions
Design & Control	Brengel and Seider, 1992	Fermentation process with model predictive control (MPC)
	Luyben and Floudas, 1994	Binary distillation with PI control
	Mohideen et al., 1996	Mixing tank and distillation column with PI control
	Kookos and Perkins, 2001	Evaporator and binary distillation with multiple PI controllers
	Bansal et al., 2002	Mixed-integer dynamic optimization of distillation with five PI controllers
	Seferlis and Georgiadis, 2004	Book, discussing many aspects of integration of design and control
	Ricardez Sandoval et al., 2008	Mixing tank with PI control using a robust modelling approach
	Sanchez-Sanchez and Ricardez-Sandoval, 2013	Single stage optimization of CSTR and ternary distillation with PI control
	Alvarado-Morales et al., 2010	Model-based optimization of bioethanol process
	Bahakim and Ricardez-Sandoval, 2014	Stochastic optimization using MPC, and application to a wastewater treatment plant using PI control
	Mansouri et al., 2016	Reactive distillation involving multiple elements
	Mehta and Ricardez-Sandoval, 2016	CSTR optimization using back-off approach and power series expansion (PSE)
	Ricardez-Sandoval et al., 2009; Sakizlis et al., 2004; Sharifzadeh, 2013; Vega et al., 2014; Yuan et al., 2012;	Reviews on integration of design and control
Control & Scheduling	Chatzidoukas et al., 2003	Optimal grade transitions for fluidized bed reactor with PI control
	Flores-Tlacuahuac and Grossmann, 2011	Non-isothermal PFR
	Zhuge and Ierapetritou, 2012	Multiproduct CSTR with PI control
	Engell and Harjunkoski, 2012	Review on integration of control and scheduling
	Chu and You, 2014b	Multiproduct CSTR with optimal control profile
	Chu and You, 2014c	Multiproduct CSTR with optimal control profile
	Zhuge and Ierapetritou, 2016	Methyl-methacrylate production with optimal control profile
Design & Scheduling	Bhatia and Biegler, 1996; Birewar and Grossmann, 1989; Castro et al., 2005; Heo et al., 2003; Lin and Floudas, 2001	Multiproduct design and scheduling of batch processes
Design, Control, & Scheduling	Terrazas-Moreno et al., 2008	Two stage optimization of methyl-methacrylate production with optimal control profile.
	Patil et al., 2015	Multiproduct process with disturbance and uncertainty, linearized process model, and frequency analysis.
	Pistikopoulos and Diangelakis, 2015	Generalized software for multi-parametric optimization. Summary of recent efforts towards integration of design, control, and scheduling.

2.2 Process Disturbances and Parameter Uncertainty

Process optimization can be complicated by considering dynamic evolution of the system subject to process disturbances and uncertainty in the model parameters. Explicitly solving an integrated optimization problem under disturbance and uncertainty is very challenging due to how quickly the problem complexity can grow. In addition, it is difficult to incorporate realistic approximations of uncertainty into the model. The optimization approach can differ, depending on if measurements are available for the parameters of interest. Parameters that are measurable can be explicitly optimized, as their values can be found, and measurement-based optimization methods can be applied (Srinivasan et al., 2002). On the other hand, unmeasurable parameters cannot be determined exactly; robust optimization methods must therefore be applied (Janak et al., 2007; Trainor et al., 2013). To generate robust solutions, decomposition algorithms can be used to simplify the problem into smaller steps (Chu and You, 2013; Heo et al., 2003; Mohideen et al., 1996). Decomposition algorithms for robust optimization typically consist of two sub-problems: a flexibility analysis and a feasibility analysis (Sakizlis et al., 2004; Sanchez-Sanchez and Ricardez-Sandoval, 2013; Seferlis and Georgiadis, 2004). In the flexibility sub-problem, a solution is chosen such that total cost is minimized and all constraints are satisfied, subject to an approximation of the process disturbances and parameter uncertainty. In the feasibility sub-problem, the solution from the flexibility sub-problem is tested for feasibility at all realizations of disturbance and uncertainty. Based on the solutions from the feasibility analysis, the approximations of disturbance and uncertainty are updated, and the algorithm returns to the flexibility problem. The algorithm typically terminates when all realizations are feasible at the given solution, though specifics of the algorithm operation can vary, depending on its implementation. Decomposition algorithms are usually used in the context of the multi-scenario approach, but they can be extended to a variety of methods.

The multi-scenario approach considers multiple different realizations of the process disturbance or parameter uncertainty in the optimization problem. A simple implementation of the multi-scenario approach considers every scenario simultaneously. However, that implementation is rarely used because it

greatly increases the problem size, which increases the computational complexity. For example, considering ten realizations simultaneously could increase the problem size by a factor of ten, and increase the computational time by an even greater factor. Therefore, although multi-scenario methods may consider a large number of scenarios, many implementations focus on a small subset of these scenarios. A "critical set" of scenarios is typically selected based on process dynamics in the feasibility analysis, where infeasible realizations are added to the critical set, so that the optimization problem can focus on searching for solutions that can accommodate those critical realizations (Mohideen et al., 1996; Seferlis and Georgiadis, 2004). The first method presented in this thesis, the critical set method, uses such an approach. During the algorithm, a critical set is built from infeasible realizations from a two-dimensional set of process disturbance and parameter uncertainty.

The second method developed in this thesis, the back-off method, is presented in this paragraph. The back-off method introduces back-off terms to the optimization, which approximate the effect of uncertainty and process disturbances, to "back off" from the optimal nominal solution without adding much complexity. The back-off method is a stochastic method, meaning it considers probabilistic representations of process disturbances and parameter uncertainty, in contrast to the discrete realizations considered by the multi-scenario approach. Thus, the back-off method makes fewer approximations and is more applicable to a variety of disturbances and uncertainty types. The back-off method for integration of design and control has been researched extensively. Early efforts involved solving dynamic systems as an improvement over steady-state optimization, using open-loop control (Figueroa et al., 1996) and PI control (Bahri et al., 1995). Advances in computational power have enabled the implementation of more challenging optimization formulations that consider the complete non-linear plant model (Kookos and Perkins, 2016; Mehta and Ricardez-Sandoval, 2016). Furthermore, stochastic simulations can be performed, to allow for statistical calculation of back-off terms (Galvanin et al., 2010; Shi et al., 2016). Although many different works make use of back-off terms in their optimization problems, the algorithms and approximations can vary significantly. In three recent works (Mehta and Ricardez-Sandoval, 2016;

Rafiei-Shishavan et al., 2017a; Rafiei-Shishavan and Ricardez-Sandoval, 2017b), power series expansion (PSE) approximations are developed for the constraints and the objective function, with respect to decision variables, process disturbance, and parameter uncertainty. The process disturbance is specified *a priori* and the parameter uncertainty is discretized to a finite number of realizations. The corresponding PSE functions are embedded within a PSE-based optimization formulation, which aims to provide the search direction for the optimal design and control scheme. To the author's knowledge, the back-off approaches presented in the literature have only been considered for integration of design and control, while the current work extends the back-off method to include scheduling.

2.3 Section Summary

The most commonly used approach for total process optimization is the sequential method, which provides a quick solution, but makes many assumptions and may not always provide a feasible solution. The integrated approach offers high quality solutions, as it can determine design, control, and scheduling simultaneously, though this method is held back by excessive computational complexity. Decomposition algorithms have been developed to break down the problem into smaller steps, and account for process disturbance and parameter uncertainty, forming the basis of the methods presented in this thesis. Both the critical set method and the back-off method are built from decomposition algorithms. The critical set method builds a set of critical (infeasible) realizations during the algorithm, and uses that critical set to determine a robust solution that can accommodate a discrete set of disturbance and uncertainty. On the other hand, the back-off method considers probabilistic representations of disturbance and uncertainty, performing process simulations to determine back-off terms, which are used to determine a robust solution that can accommodate a specified level of variability. Both methods produce robust solutions, and can be applied to the integration of design, control, and scheduling.

Many studies exist featuring the integration of design and control, for both the critical set method and the back-off method. However, very few studies consider scheduling in addition to design and

control, and this thesis aims to fill that gap in research. This thesis combines design, control, and scheduling into one optimization problem, considering disturbance and uncertainty, while making as few assumptions as possible. To the author's knowledge, the combination of all these aspects has not been previously addressed. Process disturbances and parameter uncertainty are typically very simple in many previous publications, featuring only a step change disturbance, or a small number of realizations. This thesis considers disturbance and uncertainty at the same time, with many realizations each. In the second method of this thesis, the back-off method, normal distributions are assigned to the disturbance and uncertainty, mimicking real-world variables. This is a novelty of the current work, as the back-off approach has yet to be applied to integration of design, control, and scheduling.

Chapter 3: Critical Set Methodology

This section presents the critical set methodology that is proposed to address simultaneous design, control, and short-term scheduling of multi-product plants, subject to disturbance and uncertainty. This method considers discrete realizations of uncertainty, and builds a critical set of realizations as the algorithm runs. First, the formal optimization formulation is presented for the conceptual problem. The approximations made to the original formulation are explained next, followed by the decomposition algorithmic framework developed for this method. This work has been published in Computers & Chemical Engineering (Koller and Ricardez-Sandoval, 2017a) and the ESCAPE-27 Conference Proceedings (Koller and Ricardez-Sandoval, 2017b).

3.1 Problem Definition

Consider a multiproduct processing unit that operates continuously, alternating production between various grades of a product in a wheel fashion, i.e. the sequence restarts at the beginning upon finishing. A cycle consists of transition and production regions for each product grade, therefore the total number of regions I is twice the number of grades G. During the transition region, the process set-point is changed linearly (in a ramp fashion) to the next set-point, to allow the system to smoothly transition to the new operating conditions. Following each transition region, a production region begins. The production region ends after a fixed time interval for each grade, after which the transition region begins for the next product grade. This process repeats until the demands for all grades have been satisfied. The duration of each region i is denoted as Δt_i. Additionally, since the processing unit is expected to operate continuously in a wheel fashion, the initial conditions in the first region must be equal to the final conditions in the final region, as shown in Figure 1. Note that Figure 1 is not drawn to scale, as production regions are typically far larger than transition regions.

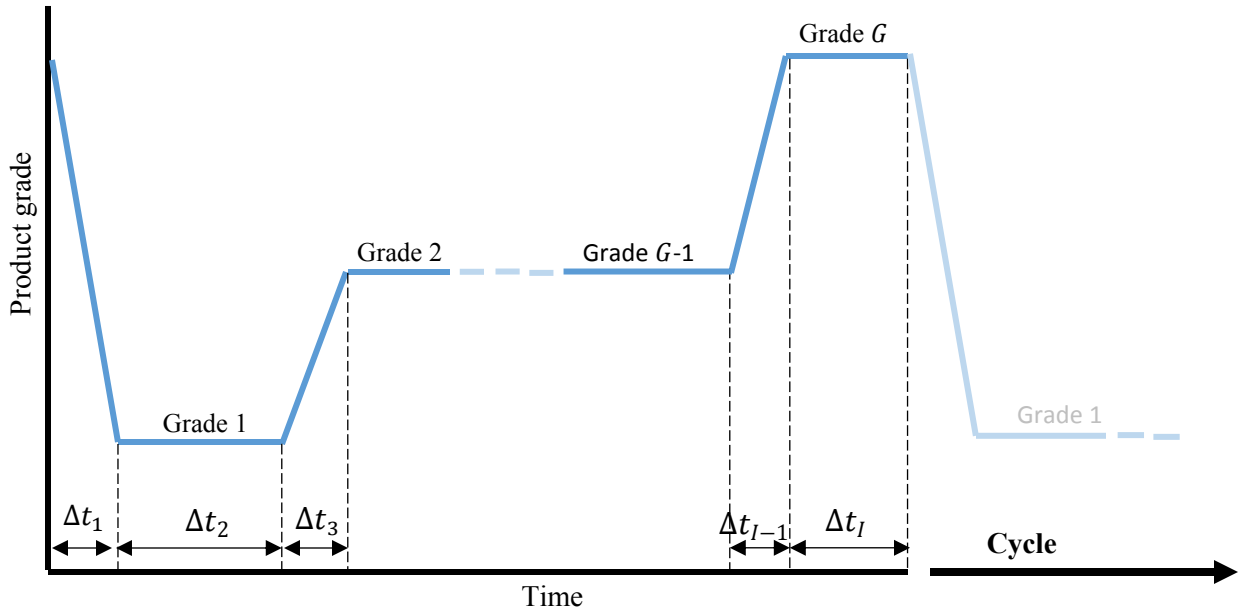

Figure 1: General production schedule of a multiproduct processing unit

This study assumes that the following are given: the actual process model representing the system's dynamic behavior, model parameters that are known with certainty (e.g. reaction rate constant, inlet flow rate), the control scheme, the required product grades and amounts to be produced and process constraints. It is also assumed that mathematical descriptions describing the process disturbances and uncertain parameters are provided. The methods presented in this work aim to provide solutions that specify the optimal equipment sizing, the optimal steady state operating conditions for each product grade, the optimal control scheme tuning parameters, the sequence of grades to be produced, and the transition times between production of each grade. The optimal solutions will be dynamically operable in the presence of disturbances and model uncertainty.

3.2 Conceptual Formulation

The explicit formulation to address the integration of design, scheduling, and control is presented in problem (1). The problem aims to minimize the total expected cost of the process z, by manipulating design, control, and scheduling decisions, while subject to time-dependent process disturbances, and uncertainty in model parameters. The design variables $\boldsymbol{\mathcal{D}}$ consist of equipment design parameters and

operating conditions. The control parameters $\boldsymbol{\mathcal{C}}$ consist of controller tuning parameters (e.g. K_c and τ_i). The scheduling variables consist of binary variables $\boldsymbol{\mathcal{S}}$ that determine the production sequence, and continuous variables $\boldsymbol{\Delta t}$ that determine the duration of each time region. For simplicity, all these variables will be referred to collectively as the decision variables $\boldsymbol{\mathcal{E}} = \{\boldsymbol{\mathcal{D}}, \boldsymbol{\mathcal{C}}, \boldsymbol{\mathcal{S}}, \boldsymbol{\Delta t}\}$. Note that each of these decisions are independent (i.e. transition durations $\boldsymbol{\Delta t}$ do not depend on control parameters or process dynamics, but are instead obtained explicitly from optimization).

$$\min_{\boldsymbol{\mathcal{E}}=\{\boldsymbol{\mathcal{D}},\boldsymbol{\mathcal{C}},\boldsymbol{\mathcal{S}},\boldsymbol{\Delta t}\}} \max_{\boldsymbol{d}(t),\boldsymbol{p}} z(\boldsymbol{x}(t), \boldsymbol{u}(t), \boldsymbol{y}(t), \boldsymbol{y^{sp}}(t), \boldsymbol{d}(t), \boldsymbol{p}, \boldsymbol{\mathcal{D}}, \boldsymbol{\mathcal{C}}, \boldsymbol{\mathcal{S}}, \boldsymbol{\Delta t}) \tag{1}$$

$s.t.$

$$\boldsymbol{f}(\boldsymbol{x}(t), \dot{\boldsymbol{x}}(t), \boldsymbol{u}(t), \boldsymbol{y}(t), \boldsymbol{y^{sp}}(t), \boldsymbol{d}(t), \boldsymbol{p}, \boldsymbol{\mathcal{D}}, \boldsymbol{\mathcal{C}}, \boldsymbol{\mathcal{S}}, \boldsymbol{\Delta t}) = \boldsymbol{0}$$

$$\boldsymbol{g}(\boldsymbol{x}(t), \boldsymbol{u}(t), \boldsymbol{y}(t), \boldsymbol{y^{sp}}(t), \boldsymbol{d}(t), \boldsymbol{p}, \boldsymbol{\mathcal{D}}, \boldsymbol{\mathcal{C}}, \boldsymbol{\mathcal{S}}, \boldsymbol{\Delta t}) \leq \boldsymbol{0}$$

$$\boldsymbol{h}(\boldsymbol{x}(t), \boldsymbol{u}(t), \boldsymbol{y}(t), \boldsymbol{y^{sp}}(t), \boldsymbol{d}(t), \boldsymbol{p}, \boldsymbol{\mathcal{D}}, \boldsymbol{\mathcal{C}}, \boldsymbol{\mathcal{S}}, \boldsymbol{\Delta t}) = \boldsymbol{0}$$

$$\boldsymbol{y^{sp}}(t) = \boldsymbol{\psi}(\boldsymbol{\mathcal{S}}, \boldsymbol{\Delta t})$$

$$\boldsymbol{d}_{lo} \leq \boldsymbol{d}(t) \leq \boldsymbol{d}_{up}$$

$$\boldsymbol{p}_{lo} \leq \boldsymbol{p} \leq \boldsymbol{p}_{up}$$

$$\boldsymbol{\mathcal{E}}_{lo} \leq \boldsymbol{\mathcal{E}} \leq \boldsymbol{\mathcal{E}}_{up}$$

$$\boldsymbol{\mathcal{S}} \in \{0,1\}$$

$$t \in [0, t_{end}]$$

The process states $\boldsymbol{x}(t)$ and its derivatives $\dot{\boldsymbol{x}}(t)$ are typically described by differential equations and are represented here by the closed-loop process model $\boldsymbol{f}$. The process constraints can take the form of inequality constraints $\boldsymbol{g}$ (physical constraints, safety constraints, quality constraints, stability constraints, and scheduling constraints) or equality constraints $\boldsymbol{h}$ (typically representing the process model algebraic equations). As shown in problem (1), the output set-points $\boldsymbol{y^{sp}}(t)$ are determined from the binary sequencing decisions $\boldsymbol{\mathcal{S}}$ and the lengths of each time region $\boldsymbol{\Delta t}$, using the function $\boldsymbol{\psi}$. The vector of process disturbances $\boldsymbol{d}(t)$ is time-varying but is assumed to be bounded by a lower limit $\boldsymbol{d}_{lo}$ and an upper limit $\boldsymbol{d}_{up}$ whereas the vector of uncertain parameters $\boldsymbol{p}$ is assumed to be time-invariant and bounded by a

lower limit $\boldsymbol{p}_{lo}$ and an upper limit $\boldsymbol{p}_{up}$. The conceptual formulation shown in problem (1) can be considered a robust optimization formulation given that the optimal solution is required to remain valid at the worst-case critical realizations of process disturbances and parametric uncertainty, thus resulting in a minimax optimization problem. Also, the formulation presented in problem (1) makes no approximations about the disturbances and the uncertain parameters, i.e. $\boldsymbol{d}(t)$ and $\boldsymbol{p}$ are defined as continuous variables encompassing an infinite number of possible realizations. Therefore, problem (1) can be classified as an infinite-dimensional mixed integer non-linear dynamic optimization problem. A large-scale problem of this type is very challenging to solve for many reasons, notably the infinite search space for disturbance and uncertain parameter domains, the combination of scheduling (binary) and continuous decisions, and the corresponding solution of differential equations at each step in the optimization. This provides motivation for the development of efficient algorithms that can circumvent these difficulties, and make the problem tractable.

In the following sub-sections, the assumptions used to make the bulk problem (1) tractable are explained. The time domain is discretized, reformulating all continuous variables into discrete points. Following that, the approximations for process disturbances and parameter uncertainty are presented, for both the Critical Set Method and the Back-Off Method. The algorithms for each method are explained, with a detailed description of each step.

3.3 Time Discretization

The problem under consideration includes time-dependent variables described by ordinary differential equations (ODEs), which are embedded within the closed-loop dynamic model of the system defined by the vector function $\boldsymbol{f}$. In addition, binary variables $\boldsymbol{S}$ are considered in the analysis to account for scheduling decisions. Thus, presence of these time-dependent and integer variables makes the overall problem a mixed-integer non-linear dynamic optimization (MIDO) problem. These types of problems can be solved using two approaches: the shooting method, and the simultaneous method. In the shooting

method, the ODEs are solved at fixed levels of the decision variables, and this is repeated multiple times in a sensitivity analysis to calculate the gradients of the objective and constraints. The gradients are then used to update the decision variables, and the process is repeated. In the simultaneous method, the ODEs are discretized, reformulating the differential equations as algebraic equations, which are then implemented into a bulk model along with the decision variables. More details about the shooting method and the simultaneous method can be found elsewhere (Biegler, 2010). The analytical gradients can be determined, and an optimal solution can be approached. In this work, the simultaneous approach has been used to reduce the computational costs and facilitate the integrated optimization of design, control, and scheduling decisions. Accordingly, the ODEs representing the closed-loop dynamic equations $\boldsymbol{f}$ are transformed into algebraic form using orthogonal collocation on finite elements, resulting in an overall problem that is a mixed-integer non-linear program (MINLP).

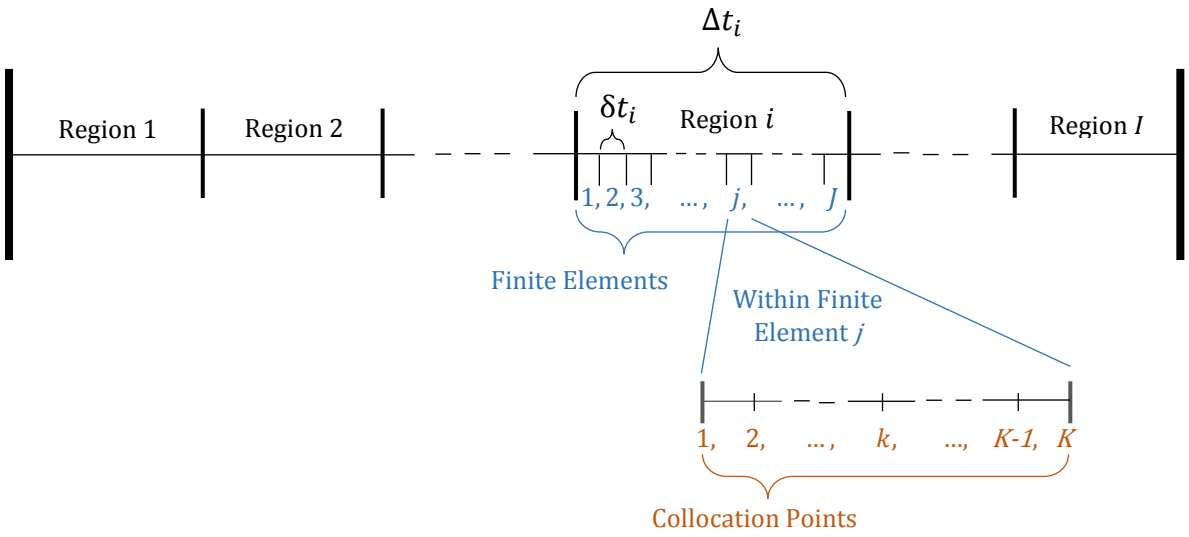

Figure 2: Visualization of time discretization into regions, finite elements, and collocation points

As shown in Figure 2, the time domain is divided into I regions, which alternate between transition regions and production regions. Each region contains J finite elements, and each finite element contains K collocation points which are spaced according to Gauss-Legendre quadrature. The duration of each region i (Δt_i) is directly determined from optimization, allowing differently sized regions to be explicitly accounted for in the MINLP formulation. As the size of each region i changes, the size of the

contained finite elements (δt_i), and their collocation points, also changes. In each region i, the size of finite elements δt_i is related to the total region size Δt_i as shown in Eq. 2.

$$\Delta t_i = J \delta t_i \quad \forall i \tag{2}$$

Based on the above descriptions, the process states $\boldsymbol{x}(t)$ can be discretized and defined as $\boldsymbol{x}_{ijk}$, as shown in Eq. 3, where i is the index of time regions, j is the index of finite elements, and k is the index of collocation points. For brevity, commas between $i, j,$ and k are omitted in most cases. All time-dependent variables (i.e. $\boldsymbol{y^{sp}}(t)$, $\boldsymbol{u}(t)$, $\boldsymbol{d}(t)$ etc.) and functions (i.e. $\boldsymbol{g}$, $\boldsymbol{h}$) are discretized in the same fashion. The value of time at each point is a function of i, j, k and the region lengths $\boldsymbol{\Delta t}$. Moreover, the time derivative for process states $\dot{\boldsymbol{x}}(t)$ can be discretized using the orthogonal collocation matrix $\boldsymbol{\mathcal{A}}$, which is defined in Appendix A, and the finite element size δt_i in each region i. Furthermore, the time-dependent variables are defined using two more indices (θ, ω), where θ and ω are the indexes corresponding to particular realizations in parameter uncertainty, and process disturbances, respectively.

$$\dot{\boldsymbol{x}}(t) = \boldsymbol{f}(\boldsymbol{x}(t), \boldsymbol{y^{sp}}(t), \boldsymbol{u}(t), \boldsymbol{d}(t), \boldsymbol{p}) \rightarrow \sum_{k'} \boldsymbol{\mathcal{A}}_{kk'} \boldsymbol{x}_{ijk'}^{\theta,\omega} = \delta t_i \, \boldsymbol{f}\left(\boldsymbol{x}_{ijk}^{\theta,\omega}, (\boldsymbol{y}^{sp})_{ijk}, \boldsymbol{u}_{ijk}^{\theta,\omega}, \boldsymbol{d}_{ijk}^{\omega}, \boldsymbol{p}^{\theta}\right)$$

$$i \in \{1,2,\dots,I\}, j \in \{1,2,\dots,J\}, k \in \{1,2,\dots,K\} \quad \omega \in \{1,2,\dots,\Omega\}, \theta \in \{1,2,\dots,\Theta\} \tag{3}$$

As shown in problem (1), the region lengths $\boldsymbol{\Delta t}$ (i.e. transition and production durations) are decision variables in the optimization. The effect of scheduling on the model equations can be seen directly in Eq. (3), which includes the finite element size δt_i for each region i directly in the process model. Also, Eq. (3) depends on the set-points of the system at each discrete point in time i, j, k (i.e. $(\boldsymbol{x}^{sp})_{ijk}$), where the corresponding set-points imposed on the process at any time point i, j, k are determined from the function $\boldsymbol{\psi}$, which depends on the binary sequencing matrix $\boldsymbol{S}$ and the region lengths $\boldsymbol{\Delta t}$, i.e. scheduling decisions. The process to obtain $(\boldsymbol{x}^{sp})_{ijk}$ is described in detail in Appendix B. This represents a novelty in the present formulation since scheduling decisions are explicitly accounted for in

the optimal design and control of multi-product systems under the effect of disturbances and uncertainty; an aspect that, to the authors' knowledge, has not been addressed in the literature.

To ensure zero- and first-order continuity between regions, and between finite elements, additional constraints (4-7) are added to the formulation. These are described in detail in Appendix A.

$$\boldsymbol{x}_{i,j,K}^{\theta,\omega} = \boldsymbol{x}_{i,j+1,1}^{\theta,\omega} \quad \forall i,j \wedge \forall(\theta,\omega) \in \boldsymbol{c} \tag{4}$$

$$\boldsymbol{x}_{i,J,K}^{\theta,\omega} = \boldsymbol{x}_{i+1,1,1}^{\theta,\omega} \quad \forall i \wedge \forall(\theta,\omega) \in \boldsymbol{c} \tag{5}$$

$$\frac{\sum_{k'} \mathcal{A}_{K,k'} \boldsymbol{x}_{i,j,k'}^{\theta,\omega}}{\delta t_i} = \frac{\sum_{k'} \mathcal{A}_{1,k'} \boldsymbol{x}_{i,j+1,k'}^{\theta,\omega}}{\delta t_i} \quad \forall i,j \wedge \forall(\theta,\omega) \in \boldsymbol{c} \tag{6}$$

$$\frac{\sum_{k'} \mathcal{A}_{K,k'} \boldsymbol{x}_{i,J,k'}^{\theta,\omega}}{\delta t_i} = \frac{\sum_{k'} \mathcal{A}_{1,k'} \boldsymbol{x}_{i+1,1,k'}^{\theta,\omega}}{\delta t_{i+1}} \quad \forall i \wedge \forall(\theta,\omega) \in \boldsymbol{c} \tag{7}$$

3.4 Approximation of Disturbance and Uncertainty

As shown in the conceptual problem (1), the process disturbances $\boldsymbol{d}(t)$ have been initially defined as bounded time-varying continuous variables, which makes problem (1) computationally challenging. To circumvent this issue, the present analysis approximates the disturbances as a set of possible functions specified *a priori*, as shown in Eq. (8). For example, the set of disturbances can take the form of sinusoidal waves with different frequency content (i.e. variability). The index ω refers to the particular realization that the disturbance can take during operation; e.g. the frequency for a sinusoidal disturbance. Similarly, the uncertain parameters $\boldsymbol{p}$ are approximated as a set of possible realizations defined *a priori*. The index θ refers to the particular realization that the parameter uncertainty vector $\boldsymbol{p}$ can take during operation, as shown in Eq. (9). To clarify, a finite list of possible values is known, but the exact value is not known. The realizations corresponding to $\omega = 0$ or $\theta = 0$ represent the nominal operating condition considered for those parameters. The sets of realizations for disturbance and uncertainty should be selected carefully, as different sets will affect the solution provided by the

algorithm. Note that increasing the number of discrete realizations is expected to have a diminishing effect on the solution (i.e. the problem is expected to converge to the same solution as the number of scenarios grows sufficiently large).

$$\boldsymbol{d}_{ijk}^{\omega} \in \left\{\boldsymbol{d}_{ijk}^{0}, \boldsymbol{d}_{ijk}^{1}, \boldsymbol{d}_{ijk}^{2}, \dots, \boldsymbol{d}_{ijk}^{\Omega}\right\} \quad \forall\, i,j,k \qquad \omega \in \{0,1,2,\dots,\Omega\} \tag{8}$$

$$\boldsymbol{p}^{\theta} \in \left\{\boldsymbol{p}^{0}, \boldsymbol{p}^{1}, \boldsymbol{p}^{2}, \dots, \boldsymbol{p}^{\Theta}\right\} \qquad \theta \in \{0,1,2,\dots,\Theta\} \tag{9}$$

In the present analysis, a critical set $\boldsymbol{c}$ is introduced in Eq. (10) as a set of (ω,θ) pairs. This set is used to define the realizations among those defined in Eq. (8) and (9) that have the most critical impact on process performance, potentially resulting in infeasibility under some conditions. Note that when a realization is referred to as critical, it is with respect to the discrete set of disturbance and uncertain realizations, which are defined *a priori*. Each set of pairs in $\boldsymbol{c}$ is a subset of all combinations of (ω,θ) considered in the disturbance and uncertain parameter sets, i.e. all ($\Omega \times \Theta$) combinations.

$$\boldsymbol{c} \subseteq \omega \times \theta = \begin{bmatrix} (0,0) & \cdots & (0,\Theta) \\ \vdots & \ddots & \vdots \\ (\Omega,0) & \cdots & (\Omega,\Theta) \end{bmatrix} \tag{10}$$

3.5 Algorithm Formulation

Using the approximations described above, the conceptual problem (1) is transformed into a minimax MINLP. Furthermore, due to the complexity of solving a minimax problem, a decomposition algorithm is implemented. As shown in Figure 3, the proposed algorithm decomposes the problem into a Flexibility Analysis and a Feasibility Analysis. These sub-problems contain the actual process model and non-linear constraints (in discrete form), and also include orthogonal collocation constraints, Eq. (4-7), which are required to ensure continuity of the process state variables $\boldsymbol{x}_{ijk}^{\theta,\omega}$ and their derivatives due to the discretization scheme employed in this work.

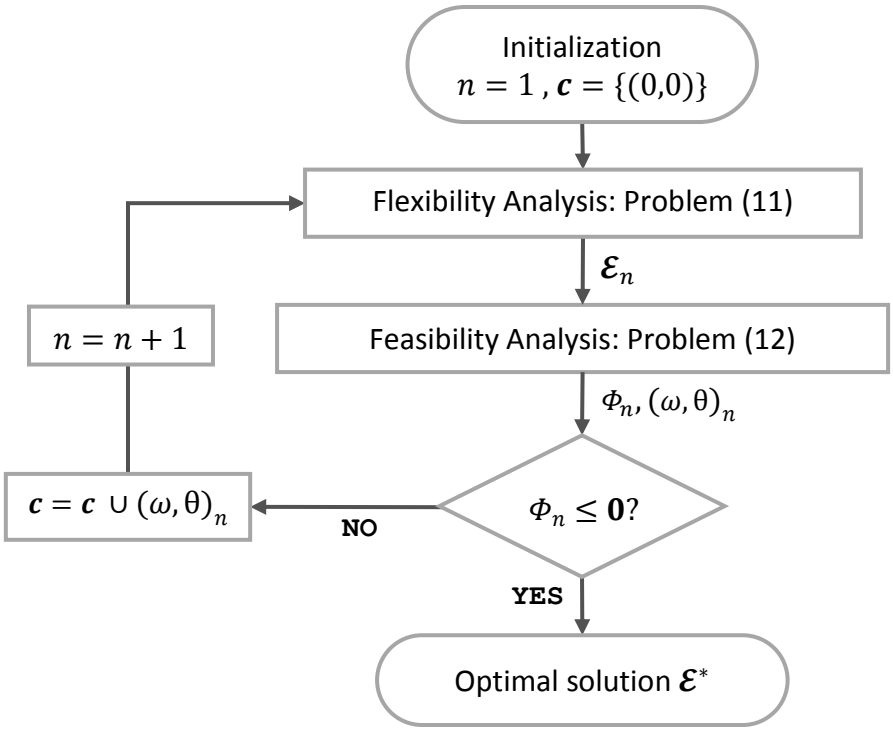

Figure 3: Critical Set Algorithm Flowchart

The flexibility analysis formulation is presented in problem (11). This problem is initialized with a critical set $\boldsymbol{c}$, which specifies the realizations of process disturbances $\boldsymbol{d}_{ijk}^{\omega}$ and parameter uncertainty $\boldsymbol{p}^{\theta}$ to be considered in the analysis. As shown in Figure 3, the critical set can be initialized in the first iteration ($n = 1$) with the corresponding nominal values (i.e. $\boldsymbol{d}_{ijk}^{0}, \boldsymbol{p}^{0}$). For a fixed critical set $\boldsymbol{c}$, the flexibility analysis searches for the design, control, and scheduling scheme that minimizes the expected cost in the objective function and accommodates the realizations considered in critical set $\boldsymbol{c}$. As shown in problem (11), each critical realization is weighted by a user-defined factor $\zeta^{\theta,\omega}$, which must be defined *a priori* and represents the likelihood or confidence that realization (θ, ω) may occur during operation.

$$\min_{\boldsymbol{\mathcal{E}}=\{\boldsymbol{\mathcal{D}},\boldsymbol{\mathcal{C}},\boldsymbol{\mathcal{S}},\boldsymbol{\Delta t}\}} \sum_{(\theta,\omega)\in\boldsymbol{c}} \zeta^{\theta,\omega} z^{\theta,\omega}\left(\boldsymbol{x}_{ijk}^{\theta,\omega}, \boldsymbol{y}_{ijk}^{\theta,\omega}, (\boldsymbol{y}^{sp})_{ijk}, \boldsymbol{\mathcal{D}}, \boldsymbol{\mathcal{C}}, \boldsymbol{\mathcal{S}}, \boldsymbol{\Delta t}\right) \tag{11}$$

$s.t.$

$$\sum_{k'} \mathcal{A}_{kk'} \boldsymbol{x}_{ijk'}^{\theta,\omega} = \delta t_i \boldsymbol{f}\left(\boldsymbol{x}_{ijk}^{\theta,\omega}, \boldsymbol{u}_{ijk}^{\theta,\omega}, \boldsymbol{y}_{ijk}^{\theta,\omega}, (\boldsymbol{y}^{sp})_{ijk}, \boldsymbol{d}_{ijk}^{\omega}, \boldsymbol{p}^{\theta}, \boldsymbol{\mathcal{D}}, \boldsymbol{\mathcal{C}}, \boldsymbol{\mathcal{S}}, \delta t_i\right), \quad \forall i, j, k \wedge \forall (\theta, \omega) \in \boldsymbol{c}$$

$$\boldsymbol{g}\left(\boldsymbol{x}_{ijk}^{\theta,\omega}, \boldsymbol{u}_{ijk}^{\theta,\omega}, \boldsymbol{y}_{ijk}^{\theta,\omega}, (\boldsymbol{y}^{sp})_{ijk}, \boldsymbol{d}_{ijk}^{\omega}, \boldsymbol{p}^{\theta}, \boldsymbol{\mathcal{D}}, \boldsymbol{\mathcal{C}}, \boldsymbol{\mathcal{S}}, \delta t_i\right) \leq \mathbf{0}\,, \quad \forall i,j,k \ \wedge \ \forall(\theta,\omega) \in \boldsymbol{c}$$

$$\boldsymbol{h}\left(\boldsymbol{x}_{ijk}^{\theta,\omega}, \boldsymbol{u}_{ijk}^{\theta,\omega}, \boldsymbol{y}_{ijk}^{\theta,\omega}, (\boldsymbol{y}^{sp})_{ijk}, \boldsymbol{d}_{ijk}^{\omega}, \boldsymbol{p}^{\theta}, \boldsymbol{\mathcal{D}}, \boldsymbol{\mathcal{C}}, \boldsymbol{\mathcal{S}}, \delta t_i\right) = \mathbf{0}\,, \quad \forall i,j,k \ \wedge \ \forall(\theta,\omega) \in \boldsymbol{c}$$

$$(\boldsymbol{y}^{sp})_{ijk} = \boldsymbol{\psi}_{ijk}(\boldsymbol{\mathcal{S}}), \quad \forall i,j,k \ \wedge \ \forall(\theta,\omega) \in \boldsymbol{c}$$

$$\boldsymbol{\mathcal{E}}_{lo} \leq \boldsymbol{\mathcal{E}} \leq \boldsymbol{\mathcal{E}}_{up}$$

$$\boldsymbol{\mathcal{S}} \in \{0,1\}$$

$$Equations\ (4) - (7)$$

The optimal solution for design, control, and scheduling returned by the flexibility problem is only guaranteed to be valid for the critical realizations considered in $\boldsymbol{c}$. Thus, a feasibility analysis is needed to ensure a robust solution that is immune to any combination of disturbance and parameter uncertainty. Therefore, the solution from the flexibility problem at the n^{th} iteration ($\boldsymbol{\mathcal{E}}_n$) is held constant and is passed to the feasibility problem. As shown in problem (12), a formal feasibility analysis optimization formulation can be formulated to search for the combination of (ω, θ) in the disturbances and uncertain parameters that produces the maximum (positive) deviation in the slack variables $\boldsymbol{\alpha}$, at any point in time i,j,k, for constraint $g_a \in \boldsymbol{g}$. Binary variables ($Y_{a,ijk}^{\theta,\omega}$) are incorporated into the formulation to indicate which realization produces the worst-case infeasibility. The problem in (12) is an integer optimization (IP) problem, as all the decisions are made on binary variables. Active set strategies (Mohideen et al., 1996) and structured singular value analysis (Trainor et al., 2013) have been proposed to solve such problems. Although the search space is finite, the problem is challenging to solve directly due to the curse of dimensionality, as the number of integer variables grows prohibitively large. However, the finite search space lends itself very well to rigorous simulations. Recent studies have used simulations to evaluate feasibility (Mansouri et al., 2016; Pistikopoulos et al., 2015; Ricardez-Sandoval, 2012; Shi et al., 2016; Zhuge and Ierapetritou, 2016). In this work, and with the aim of reducing computational complexity, process simulations are performed to calculate the values of the process variables (e.g. $\boldsymbol{x}_{ijk}^{\theta,\omega}$) and constraint violations $\alpha_{a,ijk}^{\theta,\omega}$, over the entire discrete set of process disturbances and parameter uncertainty, as shown in problem (12A).

$$\phi = \max_{\boldsymbol{Y}} \sum_{a,i,j,k,\theta,\omega} Y_{a,ijk}^{\theta,\omega}\, \alpha_{a,ijk}^{\theta,\omega} \tag{12}$$

$s.t.$

$$\sum_{k'} \boldsymbol{\mathcal{A}}_{kk'} \boldsymbol{x}_{ijk'}^{\theta,\omega} = \delta t_i * \boldsymbol{f}\left(\boldsymbol{x}_{ijk}^{\theta,\omega}, \boldsymbol{u}_{ijk}^{\theta,\omega}, \boldsymbol{y}_{ijk}^{\theta,\omega}, (\boldsymbol{y}^{sp})_{ijk}, \boldsymbol{d}_{ijk}^{\omega}, \boldsymbol{p}^{\theta}, \boldsymbol{\mathcal{D}}, \boldsymbol{\mathcal{C}}, \boldsymbol{\mathcal{S}}, \delta t_i\right) \quad \forall\, i,j,k$$

$$g_{a,ijk}^{\theta,\omega}\left(\boldsymbol{x}_{ijk}^{\theta,\omega}, \boldsymbol{u}_{ijk}^{\theta,\omega}, \boldsymbol{y}_{ijk}^{\theta,\omega}, (\boldsymbol{y}^{sp})_{ijk}, \boldsymbol{d}_{ijk}^{\omega}, \boldsymbol{p}^{\theta}, \boldsymbol{\mathcal{D}}, \boldsymbol{\mathcal{C}}, \boldsymbol{\mathcal{S}}, \delta t_i\right) = \alpha_{a,ijk}^{\theta,\omega}, \quad \forall\, a,i,j,k$$

$$\boldsymbol{h}\left(\boldsymbol{x}_{ijk}^{\theta,\omega}, \boldsymbol{u}_{ijk}^{\theta,\omega}, \boldsymbol{y}_{ijk}^{\theta,\omega}, (\boldsymbol{y}^{sp})_{ijk}, \boldsymbol{d}_{ijk}^{\omega}, \boldsymbol{p}^{\theta}, \boldsymbol{\mathcal{D}}, \boldsymbol{\mathcal{C}}, \boldsymbol{\mathcal{S}}, \delta t_i\right) = \boldsymbol{0}, \quad \forall\, i,j,k$$

$$\sum_{a,i,j,k,\theta,\omega} Y_{a,ijk}^{\theta,\omega} = 1$$

$$Y_{a,ijk}^{\theta,\omega} \in \{0,1\} \quad \forall\, \theta,\omega,a,i,j,k$$

$Equations\ (4) - (7)$

$$\Phi = \max_{\theta,\omega} \max_{a,i,j,k} \alpha_{a,ijk}^{\theta,\omega} \tag{12A}$$

$s.t.$

$$\sum_{k'} \boldsymbol{\mathcal{A}}_{kk'} \boldsymbol{x}_{ijk'}^{\theta,\omega} = \delta t_i * \boldsymbol{f}\left(\boldsymbol{x}_{ijk}^{\theta,\omega}, \boldsymbol{u}_{ijk}^{\theta,\omega}, \boldsymbol{y}_{ijk}^{\theta,\omega}, (\boldsymbol{y}^{sp})_{ijk}, \boldsymbol{d}_{ijk}^{\omega}, \boldsymbol{p}^{\theta}, \boldsymbol{\mathcal{D}}, \boldsymbol{\mathcal{C}}, \boldsymbol{\mathcal{S}}, \delta t_i\right) \quad \forall\, i,j,k$$

$$g_{a,ijk}^{\theta,\omega}\left(\boldsymbol{x}_{ijk}^{\theta,\omega}, \boldsymbol{u}_{ijk}^{\theta,\omega}, \boldsymbol{y}_{ijk}^{\theta,\omega}, (\boldsymbol{y}^{sp})_{ijk}, \boldsymbol{d}_{ijk}^{\omega}, \boldsymbol{p}^{\theta}, \boldsymbol{\mathcal{D}}, \boldsymbol{\mathcal{C}}, \boldsymbol{\mathcal{S}}, \delta t_i\right) = \alpha_{a,ijk}^{\theta,\omega}, \quad \forall\, a,i,j,k$$

$$\boldsymbol{h}\left(\boldsymbol{x}_{ijk}^{\theta,\omega}, \boldsymbol{u}_{ijk}^{\theta,\omega}, \boldsymbol{y}_{ijk}^{\theta,\omega}, (\boldsymbol{y}^{sp})_{ijk}, \boldsymbol{d}_{ijk}^{\omega}, \boldsymbol{p}^{\theta}, \boldsymbol{\mathcal{D}}, \boldsymbol{\mathcal{C}}, \boldsymbol{\mathcal{S}}, \delta t_i\right) = \boldsymbol{0}, \quad \forall\, i,j,k$$

$Equations\ (4) - (7)$

The realization with the highest objective function (i.e. the most infeasible realization) in the feasibility problem is deemed the "worst case" realization for the current iteration of the algorithm, represented as $(\omega, \theta)_n$ as shown in Figure 3. Associated with that realization is a vector of slack variables $\boldsymbol{\alpha}^{(\omega,\theta)_n}$, where positive values represent infeasible operating conditions. As shown in Problem (12A) and Figure 3, if $\Phi_n \geq 0$, i.e. any slack variables related to the "worst case" realization $(\omega, \theta)_n$ in iteration n are greater than zero, then the system is dynamically infeasible because a constraint is violated. If this is the case, then the algorithm continues to the next iteration, adding the worst case realization

$(\omega, \theta)_n$ to the critical set $\boldsymbol{c}$, and solving the flexibility problem subject to the updated critical set. Conversely, if $\Phi_n \leq 0$, i.e. all the slack variables are less than or equal to zero (i.e. all operating conditions are dynamically feasible), the algorithm terminates, and returns the current solution $\boldsymbol{\mathcal{E}}_n$ to be the most optimal solution $\boldsymbol{\mathcal{E}}^*$. This is a robust solution that is dynamically feasible for all the discrete realizations of disturbance and uncertainty that have been considered; however, it is not guaranteed to be optimal for the entire set of realizations in the disturbance and uncertain parameters. Furthermore, dynamic feasibility cannot be guaranteed for realizations other than at the discrete points in Eq. (8) and (9). Adding more realizations in the disturbances and uncertain parameter sets will improve the robustness of the resulting design, control and scheduling scheme at the expense of solving more intensive and challenging optimization problems. Structural decisions (e.g. control schemes, integer design decisions) can be considered in the flexibility analysis using additional integer variables, at the cost of increased complexity. Though the solution is robust, it may be overly conservative, especially in cases of very rare critical realizations. This can be partially remedied by careful selection of the weights $\zeta^{\theta,\omega}$ for each realization. However, robust solutions always remain conservative to some degree. Current research carried out by the authors is focused on developing new numerical approaches that can reduce the conservatism in the solution.

3.6 Application of Critical Set Method to Non-Isothermal CSTR

This section describes the case study that was adopted for the application of the critical set method. The results presented in this work were obtained using GAMS on a system running Windows 7, using an Intel® Core™ i7-2600 CPU 3.40 GHz and 8.00 GB RAM. For MINLP problems, SBB is the chosen solver. For NLP (non-linear program) and CNS (constrained non-linear system) problems, CONOPT is selected. Hence, the present analysis accepts locally optimal solutions. Preliminary analysis showed that these solvers provided better performance than other solvers (e.g. DICOPT, IPOPT) for this case study.

The approach described in the previous section has been applied to a non-isothermal continuous stirred tank reactor (CSTR), which is shown in Figure 4. This case study is intended to be of similar complexity to the case studies used in other works on integrated design, control and/or scheduling optimization (Mehta and Ricardez-Sandoval, 2016; Patil et al., 2015; Terrazas-Moreno et al., 2008; Zhuge and Ierapetritou, 2016, 2012). The reactor has constant volume, due to an overflow outlet. The reactor temperature is not constant with respect to time, but it is uniform within the reactor, as the reactor is assumed to be well mixed. Multiple grades of product B must be produced via an irreversible first-order reaction that converts reactant A into product B. The various product grades are produced one at a time, i.e. in a wheel fashion. Scheduling decisions include the production sequence and the transition durations (i.e. region lengths $\boldsymbol{\Delta t}$) between product grades. During the production regions, deviation from the concentration set-point is penalized in the cost function.

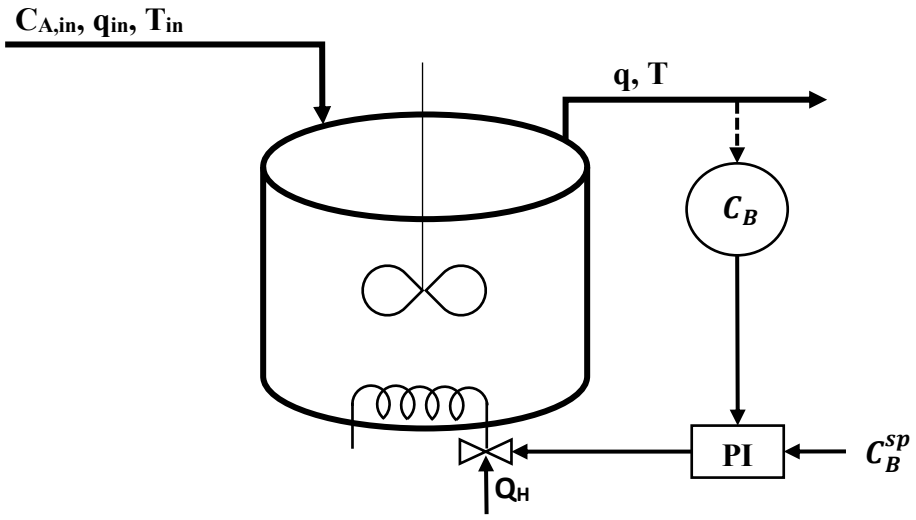

Figure 4: Schematic of CSTR system

As shown in Figure 4, the feed to the reactor consists entirely of species A, at a concentration of $C_{A_{in}}$ (3.0 mol/L), flow rate q_{in}, and temperature T_{in} (40°C). The feed must be converted to product B via an exothermic reaction. The reaction is assumed to follow first order Arrhenius kinetics as in Eq. (13).

$$r_A = k_o C_A \exp\left(\frac{-E_R}{R\,T}\right) \tag{13}$$

where C_A is the concentration of species A in the reactor, k_o is the pre-exponential constant ($1.3\ s^{-1}$), R is the gas constant ($8.3144\ J \cdot mol^{-1} \cdot K^{-1}$), T is the temperature in the reactor, and E_R is the activation energy of the reaction ($20000\ J/mol$). The dynamic behavior of the state variables $\boldsymbol{x}_{CSTR} = \{T, C_B\}$ is described in Eq. (14)-(15). Equations are shown in continuous form and have been discretized before implementation as shown in Section 3. Orthogonal collocation for this case study is discussed further in Appendix A.

$$\frac{dT}{dt} = \frac{q_{in}(T_{in} - T)}{V} + \frac{\Delta H_R k_o (C_{A_{in}} - C_B)}{\rho\, C_P} \exp\left(\frac{-E_R}{R\,T}\right) - \frac{Q_H}{\rho C_P V} \tag{14}$$

$$\frac{dC_B}{dt} = k_o\left(C_{A_{in}} - C_B\right) \exp\left(\frac{-E_R}{R\,T}\right) + \frac{q_{in} C_B}{V} \tag{15}$$

where C_B is the concentration of species B (product) in the reactor, V is the volume of liquid in the reactor, ΔH_R is the heat of reaction ($4780\ J/mol$), ρ is the density of the liquid in the reactor ($1\ kg/L$), C_P is the specific heat capacity of the liquid ($4.1813\ J \cdot g^{-1} \cdot K^{-1}$), and Q_H is the rate at which heat is added/removed to the system.

The control scheme consists of a PI controller that uses the heating rate Q_H to control the product concentration C_B at the outlet. As shown in Eq. (16), the concentration set-point is denoted by C_B^{sp} whereas the controller parameters are represented by the proportional gain K_c, and the integral time τ_i. The steady state (nominal) heating rate is $\overline{Q_H}$. Due to large differences between typical values of $C_B(t)$ and $Q_H(t)$, the value of K_c is scaled by 10^6 (not shown), for clarity of results.

$$Q_H(t) = \overline{Q_H} + K_C\left(C_B^{sp} - C_B(t)\right) + \frac{K_c}{\tau_i}\int_0^t \left(C_B^{sp} - C_B(t')\right) dt' \tag{16}$$

For safety reasons, the temperature inside the reactor must be maintained between 0°C and 400°C during operation, as shown in Eq. (17). Additionally, the rate of change in the manipulated variable (heat input Q_H) is constrained, as shown in Eq. (18), to prevent drastic changes in the heat input. This case study considers five set-points C_B^{sp} shown in Eq. (19), which are also referred to as set-points A, B, C, D, E

respectively. To simplify the present analysis, the demand for each grade is assumed to be constant and equal for this case study. However, this is not required by the methodology and can be extended to consider unequal production of different product grades. As described in Section 2, there is a corresponding transition and production region for each set-point. Therefore, the total number of regions I is equal to 10 (i.e. there are 5 transition regions $i_t \in \{1, 3, 5, 7, 9\}$ and 5 production regions $i_p \in \{2, 4, 6, 8, 10\}$). As described in Section 3.3, all variables are discretized into regions i, finite elements j, and collocation points k. In this case study, each region i contains 100 finite elements, i.e. J=100. Within each finite element, there are K=5 collocation points, including the boundary points. The number of finite elements and collocation points were selected *a priori* based on a preliminary analysis of computational effort against accuracy in the solution.

To account for grade transitions, the duration Δt_i of each region i is an optimization variable in the transition regions (odd numbered regions), and is bounded as shown in Eq. (20) to resemble a real process where there may be scheduling/operational limits imposed on time. In production regions (even numbered regions), the region duration is fixed at 4,000 seconds. As discussed in Section 3.2.3, additional constraints are necessary to ensure zero- and first-order continuity between finite elements and regions. Details on the implementation for this case study are discussed in Appendix A.

$$0°\text{C} \leq T(t) \leq 400°\text{C} \tag{17}$$

$$-50\ \text{kW/s} \leq \frac{dQ_H(t)}{dt} \leq 50\ \text{kW/s} \tag{18}$$

$$C_B^{sp} \in \{0.7, 0.9, 1.2, 1.5, 1.7\}\ L/mol \tag{19}$$

$$10\ s \leq \Delta t_i \leq 300\ s \qquad i \in i_t \tag{20}$$

The objective of the optimization problem is to minimize total cost of the process. The total cost z_{CSTR} shown in Eq. (21) is assumed to be the sum of capital cost, scheduling cost, and variability cost. Capital cost is a direct function of reactor volume V, scheduling cost is a function of the length of each

transition region Δt_i, and variability cost is a function of the integral of squared error ISE_i of the outlet product concentration in each production region. Gaussian quadrature is used in place of a traditional integral to calculate ISE_i, as shown in (22), where φ_k is the Gaussian weight of each discrete point. Note that the weights assigned to each of the cost function terms were arbitrarily selected.

$$z_{CSTR} = 10V + 20\sum_{i\in i_t}\Delta t_i \; + 10\sum_{i\in i_p} ISE_i \tag{21}$$

$$ISE_i = \sum_j \sum_{k\notin\{1,K\}} \frac{\varphi_k}{2}\delta t_i \left(C^{sp}_{B_{ijk}} - C_{B_{ijk}}\right)^2 \qquad \forall\, i \tag{22}$$

The decision variables for this case study are the reactor volume V (design decisions), the controller tuning parameters K_C and τ_i (control decisions) and the sequence of production (binary matrix $\boldsymbol{\mathcal{S}}$) and the transition region lengths $\boldsymbol{\Delta t}$ (scheduling decisions). The lengths of the production regions are fixed at 4000 s, based on product demand. Although such short production periods may not be realistic, the weighting of the production regions can be manipulated to mimic the effect of a longer production region, without increasing the problem complexity. The flexibility analysis also includes constraints on the production sequence such that only one grade is produced at a time (Eq. (23)), and that all grades are produced by the end of the time horizon (Eq. (24)). Due to the repeating production schedule as mentioned in Section 3.1, there are many production sequences which are identical (e.g. A-B-C-D-E and B-C-D-E-A, etc.). Therefore, to reduce the computational costs, the first set-point is fixed so it is always the first grade ($0.7\ mol/L$).

$$\sum_{g'} \mathcal{S}_{g,g'} = 1 \qquad \forall g \tag{23}$$

$$\sum_{g} \mathcal{S}_{g,g'} = 1 \qquad \forall g' \tag{24}$$

3.6.1 Scenario A: Comparison to Nominal Optimization

In this scenario, the results from two implementations are compared. The first problem (*Scenario A1*) considers that the selected process disturbance, i.e. the inlet flow rate q_{in}, is set to its nominal operating condition while the second problem (*Scenario A2*) considers an oscillating inlet flow rate q_{in}. In both problems, design, control, and scheduling are optimized simultaneously using the proposed algorithm. The purpose of this scenario is to illustrate the effect that disturbance has on the optimal design, control, and scheduling.

As shown in Eq. (25), the inlet flow rate q_{in} is assumed to oscillate around a nominal point $q_{in_{nom}}$ (0.4 L/s) following a sinusoidal wave with an amplitude of $q_{in_{amp}}$ (0.08 L/s),. The oscillation frequency ν is assumed to be an unknown parameter chosen from a discrete set of frequencies shown in Eq. (26). Accordingly, $\omega \in \{0,1,2,\dots,10\}$ refers to a particular disturbance realization, similar to Eq. (8) in Section 3.4. All realizations are assumed to be equally likely, i.e. $\zeta^{\omega} = 1/11$. In *Scenario A1*, the inlet flow rate is assumed to be equal to the nominal value, i.e. $\nu = 0$.

$$q_{in} = q_{in_{nom}} + q_{in_{amp}} \sin(\nu t) \tag{25}$$

$$\nu \in \{0, 0.001, 0.002, 0.004, 0.007, 0.01, 0.02, 0.04, 0.07, 0.1, 0.2\}\ s^{-1} \tag{26}$$

Table 2: Summary of Results from Scenario A

Scenario	*Scenario A1*	*Scenario A2*
Optimal Process Cost ($)	177	388
CPU Time (s)	494	4,649 (four iterations)
Reactor Volume $V(L)$	13.6	15.4
Controller K_C, τ_i	1.95, 146	5.00, 346
ISE of concentration	1.22	17.63
Production sequence	A-B-C-E-D	A-C-E-D-B
Transition durations $\boldsymbol{\Delta t}$ (s)	46.2, 10.0, 18.3, 63.3, 10.0	33.9, 66.5, 119, 25.0, 46.6
Critical set c	$\boldsymbol{c} = \{(\omega = 0)\}$	$\boldsymbol{c} = \{(\omega = 0), (\omega = 5), (\omega = 2), (\omega = 4)\}$

The results for these implementations are summarized in Table 2. *Scenario A1* requires a single flexibility problem to generate a solution subject to nominal conditions. *Scenario A2* requires four iterations of the proposed algorithm to converge to an optimal solution that is feasible for all the realizations considered. Note that the solution provided by *Scenario A1* does not remain feasible under all realizations of process disturbance (not shown for brevity). The size of the flexibility analysis (11) in *Scenario A2* grows in each successive iteration, because the problem must be solved over all realizations in the critical set, which is expanded following each feasibility analysis, as shown in Figure 3. In the final iteration of the algorithm for *Scenario A2*, the flexibility problem consisted of 119,529 equations and 89,553 variables, while the feasibility simulations consisted of 21,507 equations and variables. The use of simulations in the feasibility analysis is justified, as the formal optimization in (12) would have contained 50,000 binary variables, resulting in a nearly intractable IP problem. Conversely, the computational time for the feasibility analysis simulations in (12A) required only 25 seconds.

The problem size of *Scenario A1* is smaller than that of *Scenario A2*, consisting of 46,519 equations and 36,543 variables. As expected, the CPU time is much higher for *Scenario A2* (at least one order of magnitude) since the problem is larger and requires multiple iterations. As expected, the total process cost and ISE are higher in *Scenario A2,* due to the presence of disturbance. Note that both scenarios returned different scheduling solutions, in terms of sequencing and transition durations, aside from the starting point (which was fixed). *Scenario A2* has lower transition durations, to account for process disturbances. Control parameters are also significantly different, due to the differences in scheduling. Furthermore, the reactor volume is 13% larger in *Scenario A2* than in *Scenario A1*. These results highlight the importance of taking scheduling decisions into account while performing the optimal design of a multiproduct system. The concentration profile from each of the scenarios is displayed in Figure 5, showing nominal operation with no disturbance (*Scenario A1*) and disturbed operation with critical disturbance (*Scenario A2*). The differences in sequence, transition times, and control tuning can be observed.

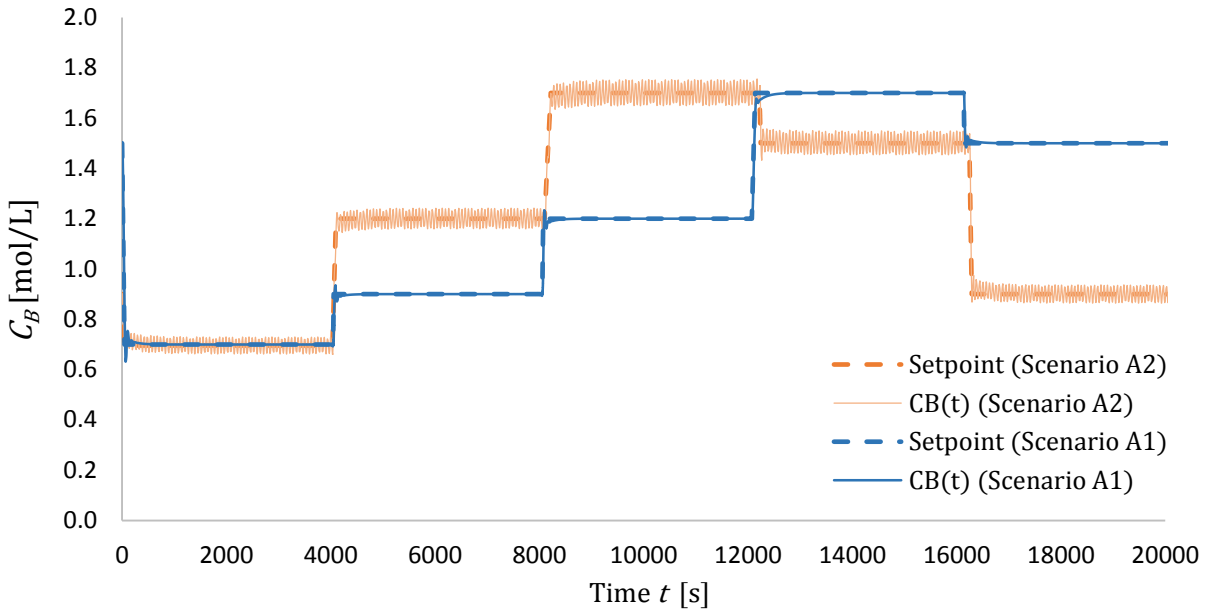

Figure 5: Concentration profile comparison for Scenario A

3.6.2 Scenario B: Comparison to Sequential Method

In this scenario, results from the proposed methodology (*Scenario B1*) are compared to the results from the sequential method (*Scenario B2*) and the sequential method with overdesign factors (*Scenario B3*). The purpose of this scenario is to compare these competing methodologies in terms of solution quality and computational time. The problems are solved subject to the process disturbance described in the previous scenario. Additionally, uncertainty is considered for two parameters in this process: heat of reaction ΔH_R, and activation energy E_R. The corresponding value of these parameters is determined by the uncertainty realization $\theta \in \{0,1,2,3,4\}$ as shown in Table 3. Note that the complexity of the problem increases since all the combinations of disturbance (11 realizations) and uncertainty (5 realizations) are considered, resulting in 55 possible realizations. The decomposed algorithm is initialized with $\omega = 0$ (see Eq. (25)) and $\theta = 0$, to represent nominal values.

Table 3: Uncertainty Realizations for Scenario B

Realization θ	Heat of Reaction ΔH_R (J/mol)	Activation Energy E_R (J/mol)
0	5000	20000
1	6000	21000
2	4000	19000
3	4000	21000
4	6000	19000

For *Scenario B2 and B3*, the sequential method consists of three consecutive sub-problems (i.e. design, control, and scheduling), where the solution from each sub-problem is fixed in the calculations and passed to the next sub-problem; hence, there is no interaction between the different sub-problems. Due to the independence of the sub-problems in the sequential method, it is much less complex than the integrated approach. Once a solution is determined using the sequential method, the solution is tested against the full set of realizations of disturbance and uncertainty. The worst-case solution (i.e. the most infeasible solution) is returned as the final solution. This is to provide a fair comparison to the proposed method, which also returns the solution that accommodates the worst-case (critical) realizations in ω and θ. The solution obtained from the sequential approach (*Scenario B2*) contained multiple infeasible realizations. Hence, an overdesign factor of 1.5 was applied to the reactor volume in *Scenario B3* to prevent dynamic infeasibility, based on a preliminary analysis of overdesign factors ranging from 1.1 to 2.0, in increments of 0.05. With the overdesigned sequential approach (*Scenario B3*), all the realizations become feasible and comparison to the integrated approach is possible.

For *Scenario B1*, five iterations of the proposed algorithm are required before convergence is met. Results following the flexibility problem from each iteration are summarized in Table 4. The critical set $\boldsymbol{c}$ is initialized with the nominal point $(0,0)$, and a new realization in the disturbance and uncertain parameters is added to the critical set in each iteration. The effects of the expanding critical set can be seen as the problem size increases and the solution changes slightly in each iteration. Given that the present approach uses the solution from the previous iteration to initialize the problem at the current iteration, then a direct relationship between computational costs and problem size shall not be expected

since it also depends on other factors such as initial conditions and non-linearities. In the final iteration, all realizations are identified as feasible in the feasibility analysis, so the algorithm is terminated, and the design, control and scheduling scheme corresponding to that iteration is reported as the optimal solution ($\boldsymbol{\mathcal{E}}^*$) as shown in Figure 3.

Table 4: Summary of Flexibility Analyses in Scenario B1

Iteration	Critical Set	Solution	CPU Time	# of equations # of variables
1	$\boldsymbol{c}$ = {(0,0)}	V = 13.48 K_c, τ_i = 2.11, 823 Sequence: A-B-C-D-E $\boldsymbol{\Delta t}$ = 88, 52, 40, 48, 10	183 s	23,269 18,293
2	$\boldsymbol{c}$ = {(0,0), (8,1)}	V = 18.51 K_c, τ_i = 5.00, 130 Sequence: A-B-C-D-E $\boldsymbol{\Delta t}$ = 114, 10, 10, 10, 10	249 s	41,524 31,548
3	$\boldsymbol{c}$ = {(0,0), (8,1), (9,1)}	V = 18.54 K_c, τ_i= 5.00, 137 Sequence: A-B-C-D-E $\boldsymbol{\Delta t}$ = 101, 40, 10, 10, 10	469 s	59,779 44,803
4	$\boldsymbol{c}$ = {(0,0), (8,1), (9,1), (7,1)}	V = 18.56 K_c, τ_i= 5.00, 251 Sequence: A-B-E-D-C $\boldsymbol{\Delta t}$ = 52, 10, 99, 10, 10	1271 s	78,034 58,058
5	$\boldsymbol{c}$ = {(0,0), (8,1), (9,1), (7,1), (5,1)}	V = 18.89 K_c, τ_i = 5.00, 764 Sequence: A-B-E-D-C $\boldsymbol{\Delta t}$ = 155, 51, 281, 35, 28	920 s	96,289 71,313

Table 5 presents the results obtained from *Scenario B*. As shown in this table, the optimal process cost provided by the integrated approach (*Scenario B1*) is 17% lower than the solution provided by the overdesigned sequential approach (*Scenario B3*), and every component of the cost function is also lower. *Scenario B2* has the lowest process cost out of all scenarios considered though it returns a dynamically infeasible design. The computational cost of the integrated approach (*Scenario B1*) is approximately three times higher than that of *Scenario B3*, due to the increased complexity of the integrated problem, as mentioned above.

Table 5: Summary of Results from Scenario B

Method	*Integrated approach (Scenario B1)*	*Sequential approach (Scenario B2)*	*Overdesign Sequential approach (Scenario B3)*
Optimal Process Cost ($)	607	385 (Infeasible)	735
Capital Cost ($)	189	150	225
Transition Cost ($)	110	27	119
Variability Cost ($)	308	208	391
CPU Time (s)	4,147 (5 iterations)	1,016 (sum of all stages)	801 (sum of all stages)
Reactor Volume $V(L)$	18.9	15.0	22.5
Controller K_C, τ_i	5.00, 764	5.00, 137	5.00, 456
Production sequence	A-B-E-D-C	A-B-D-E-C	A-C-B-E-D
Transition times $\boldsymbol{\Delta t}$ (s)	155, 51.0, 281, 35.4, 27.9	39.5, 20.9, 34.9, 10.1, 29.1	284, 178, 55.8, 48.4, 32.6
Critical set $\boldsymbol{c}$	$\boldsymbol{c}$ = $\{(0,0),(8,1),(9,1),(7,1),(5,1),(9,3)\}$	Dynamically Infeasible	Dynamically Feasible

As shown in Table 5, the controller integral time is significantly different for each approach, and the lower variability cost indicates that the integrated approach offers better set-point tracking performance than *Scenario B3*. The reactor volume is also lower in the integrated approach, leading to a 16% lower design cost compared to *Scenario B3*. Note that the reactor volume from the integrated approach (V = 18.9) is only 26% greater than *Scenario B2* (V = 15), which was found to be dynamically infeasible. This indicates that by integrating design with control and scheduling decisions, the reactor volume was able to remain relatively low without resulting in dynamically infeasible (invalid) designs in the presence of disturbance and parameter uncertainty. Additionally, it is likely that reactor volume has a large effect on process dynamics; thus, the reactor sizing in the sequential approach is suboptimal because it is determined in the first stage of optimization (before control and scheduling have been determined). Note that the production sequence and transition durations are also significantly different. This is a clear indication that scheduling decisions are affected by design and control decisions, thus motivating the need for integration of these three aspects. *Scenario B1* and *Scenario B3* are feasible over all realizations of process disturbance and uncertainty, while *Scenario B2* is dynamically infeasible. The concentration

profiles from *Scenario B1* (integrated approach) and *Scenario B3* (overdesign sequential approach) are shown in Fig. 6, where differences can be observed in production sequence, transition times, process variability and controller tuning.

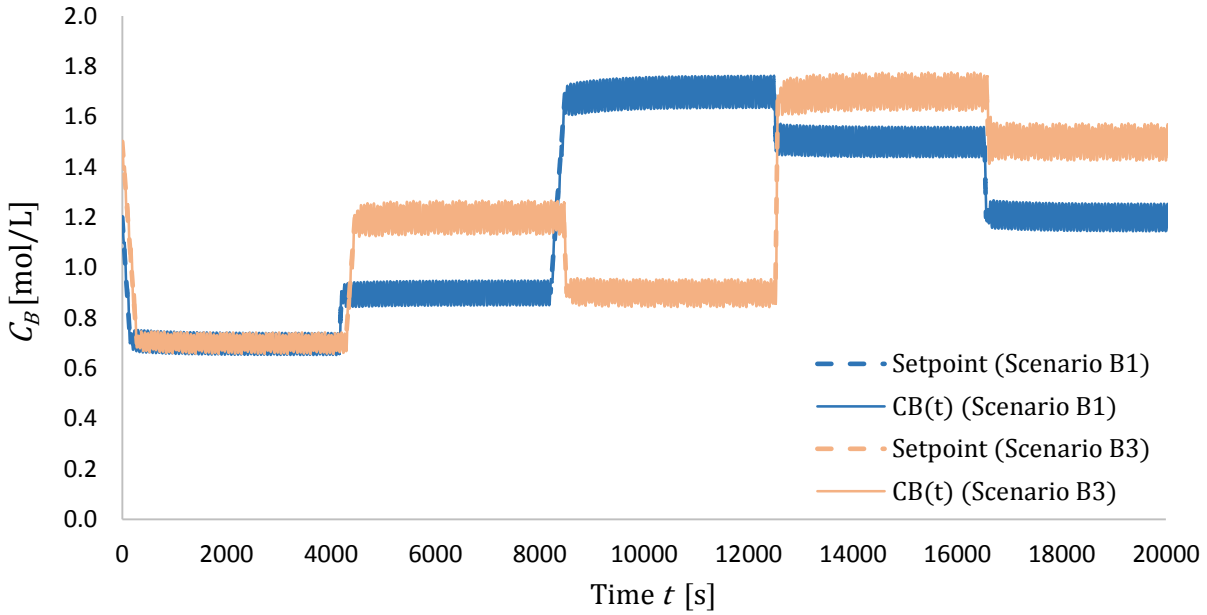

Figure 6: Concentration profile comparison for Scenario B

In Fig. 7, it can be observed that the temperature from the integrated approach (*Scenario B1*) remains within the corresponding limits specified for this variable (see Eq. (17)), and oscillates as closely as possible to the limit. For *Scenario B2* (the unmodified sequential approach), the temperature surpasses the upper bound, resulting in infeasible operating conditions. In Fig. 8, the profile of the manipulated variable (heat input) in *Scenario B1* is illustrated. Similar to temperature, the heat input oscillates to correct for changes in the disturbances and the uncertain parameters (ΔH_R and E_R), and no drastic changes are observed.

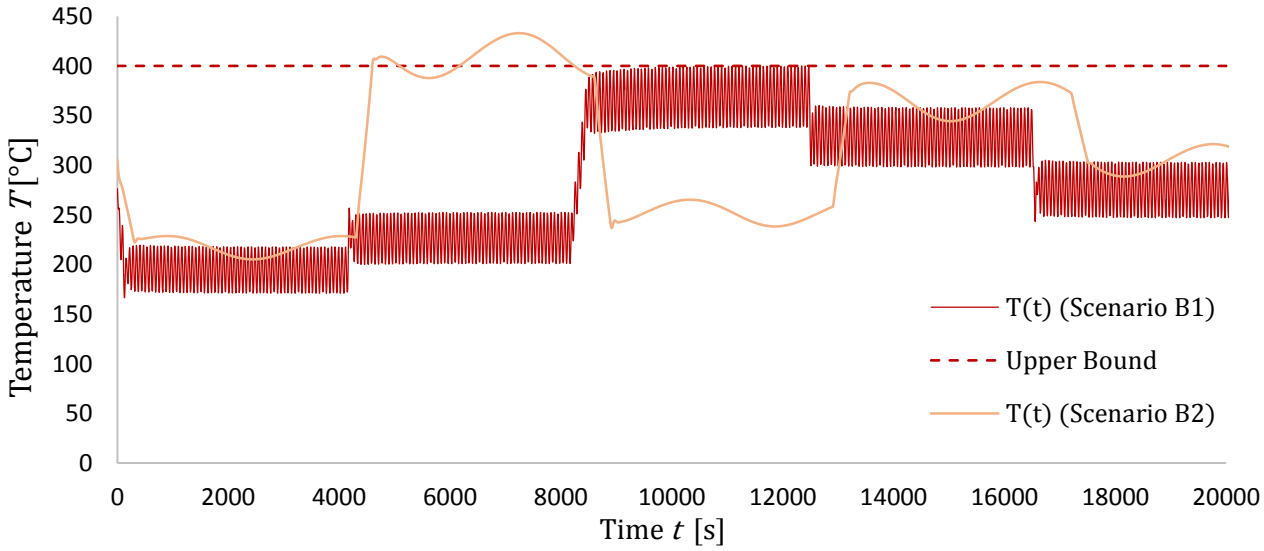

Figure 7: Reactor temperature profiles from Scenario B

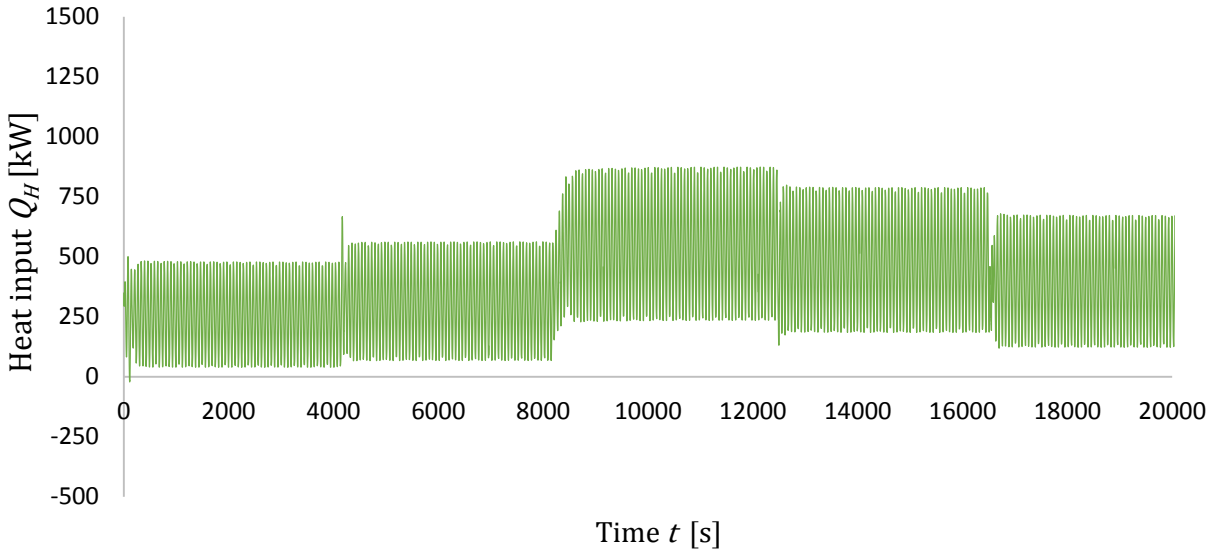

Figure 8: Heat input profile from Scenario B1

The progression of the algorithm in the integrated approach (*Scenario B1)* can be observed in Figure 9, which displays the maximum infeasibility (Φ_n) in temperature constraints detected from the feasibility analysis at each iteration n. Infeasibility starts out high (55 °C above upper bound), and then generally decreases with each iteration, although that is not guaranteed. The algorithm terminates after the fifth iteration, when no infeasibilities were detected, i.e. $\Phi \leq 0$.

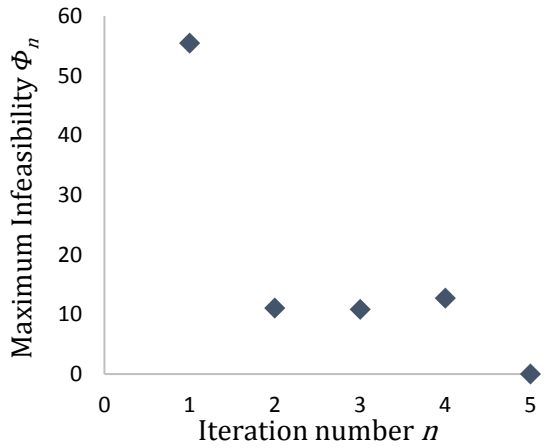

Figure 9: Algorithm convergence for Scenario B1

3.6.3. Cost Function Sensitivity Analysis for Scenario B

In this scenario, a sensitivity analysis was performed on the weights assigned to each term in the objective function (Eq. 21) to determine the effect on the solution obtained from Scenario B. Three sensitivity scenarios are considered in this analysis. In each of the scenarios, a 10% increase is applied to a coefficient in the objective function, either capital cost weight, scheduling cost weight or variability cost weight. To simplify the analysis, each sensitivity problem is initialized with the optimal solution provided by the critical set method in *Scenario B1*. Results from this analysis are displayed in Table 6.

Table 6: Summary of Sensitivity Analyses for Scenario B

Method	*Increased Capital Cost Weight*	*Increased Scheduling Cost Weight*	*Increased Variability Cost Weight*
Total Process Cost ($)	626	618	638
Capital Cost ($)	208	189	189
Transition Cost ($)	110	121	110
Variability Cost ($)	308	308	339
Reactor Volume $V(L)$	18.9	18.9	18.9
Controller K_C, τ_i	5.00, 764	5.00, 765	5.00, 761
Production sequence	A-B-E-D-C	A-B-E-D-C	A-B-E-D-C
Transition times $\boldsymbol{\Delta t}$ (s)	155, 51.0, 281, 35.4, 27.9	155, 51.0, 281, 35.1, 27.3	155, 51.0, 281, 35.7, 28.2

As shown in Table 6, all three analyses returned a solution that is nearly identical to that obtained for *Scenario B1* with negligible differences in transition times and controller integral time. The observed changes in the total process cost of 3.03%, 1.81% and 5.11%, respectively, are fully explained by the differences in cost weights, i.e. a 10% increase in the capital cost weight returned a 10% increase in the capital cost. These results show that the solution obtained in *Scenario B1* is robust (i.e. insensitive) to small changes in the weights specified in the cost function.

3.7 Application of Critical Set Method to Isothermal PFR

To further test the proposed critical-set method, the simultaneous design, control and scheduling of a plug flow reactor (PFR) is determined. The PFR, adopted from the case study described by Flores-Tlacuahuac and Grossmann (2011), consumes reactant A via an irreversible second-order reaction. The reactor is assumed to be isothermal due to an ideal heating/cooling jacket, i.e. the rate constant k_o is constant. The reactor has a total length L and a flow rate q_{in}. The system is described by the PDE and boundary conditions in Eq. (27), where C_A is the reactant concentration as a function of length x and time t. Radial effects are assumed to be negligible. The diffusion coefficient D_A (10 m^2/s) and the cross-sectional area A_c (0.785 m^2) are known. A schematic of the PFR system is shown in Figure 10.

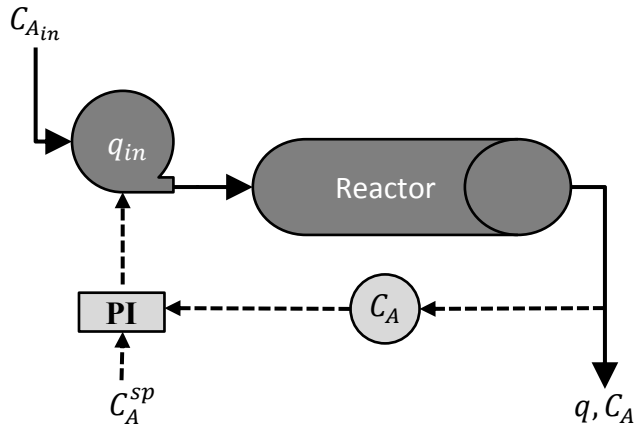

Figure 10: Schematic of PFR system

$$\frac{\partial C_A}{\partial t} = D_A \frac{\partial^2 C_A}{\partial x^2} + \frac{q_{in}}{A_c}\frac{\partial C_A}{\partial x} - k_o C_A^2 \tag{27}$$

$s.t.$

$C_A(x, t = 0) = C_{A,initial}$

$C_A(x = 0, t) = C_{A.inlet}$

$$\left.\frac{\partial C_A(x,t)}{\partial x}\right|_{x=L} = 0$$

Different product grades are produced on a cyclic schedule, and demand for each grade is assumed to be equal. The outlet concentration of reactant A is controlled by a PI controller that manipulates the input flow rate q_{in}. Due to physical limitations of the pump, the inlet flow rate q_{in} must remain between 0.25 and 10 m^3/s at all times. This case study considers five set-points $C_A^{sp} \in$ {50, 56, 63, 71, 80}, which are referred to as {A, B, C, D, E}, respectively. Therefore, the total number of regions *I* is equal to 10, identical to the CSTR case study (i.e. there are 5 transition regions $i_t \in$ {1, 3, 5, 7, 9} and 5 production regions $i_p \in$ {2, 4, 6, 8, 10}). The number of finite elements *J* in each region is chosen to be 40, and the number of collocation points *K* is set to 5. These values were selected based on a preliminary analysis of computational effort against accuracy in the solution. The lengths of transition regions Δt_i are optimization variables in the analysis, subject the same bounds as Eq. (20), while the length of each production regions is fixed at 360 s. Time-dependent variables are discretized in time, and spatially-dependent variables are also discretized along the spatial domain. The number of spatial nodes is chosen to be 11, and finite difference equations are used at the nodes, as shown in Flores-Tlacuahuac and Grossmann (2011). As shown in Eq. (28), the cost function z_{PFR} to be minimized is the sum of capital cost (reactor length), scheduling cost (duration Δt_i of each transition region), and variability cost (integral of squared error ISE_i of outlet concentration in each production region).

$$z_{PFR} = 10L + \sum_{i \in i_t} \Delta t_i + \frac{1}{100}\sum_{i \in i_p} ISE_i \tag{28}$$

The decision variables for this case study are the reactor length L (design decision), the controller tuning parameters K_c and τ_i (control decisions), and the sequence of production $\boldsymbol{S}$ and the transition durations $\boldsymbol{\Delta t}$ (scheduling decisions). There are constraints on the production sequence such each grade is produced once in the time horizon, and only one grade is produced at a time. The constraints on the inlet flow rate q_{in} are also considered in the analysis. Due to the wheel-like production schedule, many sequences are not unique (e.g. A-B-C-D-E and D-E-A-B-C, etc.). To remedy this, the first set-point is fixed to be the highest grade (80 mol/L).

The process is disturbed by the inlet reactant concentration $C_{A.inlet}$, which oscillates around a nominal point of 100 mol/L, following a sinusoidal wave with an amplitude of 15 mol/L. The oscillation frequency ν is unknown, but is assumed to belong to a discrete set of values {0, 1, 2, 5, 8, 10, 12, 14, 16, 18, 20}×10^{-3} rad/s, as indicated by the index $\omega \in \{1, 2, 3, 4, 5, 6, 7, 8, 9, 10, 11\}$. All realizations are assumed to be equally likely. Discrete parametric uncertainty is considered for the reaction rate constant $k_o \in$ {1.00, 0.90, 0.95, 1.05, 1.10}×10^{-4} L/(mol·s). The particular realization is indicated by $\theta \in \{1, 2, 3, 4, 5\}$. The analysis considers all combinations of disturbance (11 realizations) and uncertainty (5 realizations), for a total of 55 possible realizations. The algorithm is initialized with $\omega = 1$ and $\theta = 1$ (i.e. $\Omega = 0$ rad/s and $k_o = 10^{-4}$ L/(mol·s)) to represent nominal values.

3.7.1 Scenario C: PFR Comparison to Sequential Method

The present case study was implemented on GAMS and solved using an Intel® Core™ i7-2600 CPU 3.40 GHz and 8.00 GB RAM. Solvers used were SBB and CONOPT for the flexibility and feasibility analysis, respectively; these solvers were selected based on a preliminary analysis. The comparison case of the sequential method was generated with an overdesign design factor; reducing reactor length by one-third. This may seem backwards, but it does indeed allow for a robust solution. Had the reactor length not been reduced, the required flow rate q_{in} to produce the highest grade (which

demands low residence time) would have been beyond the upper bound of 10 m^3/s once disturbance and uncertainty were considered in the system.

The results obtained from each of the approaches are displayed in Table 7. As shown in this table, the total cost provided by the integrated approach *(Scenario C1)* is 46 % lower than that returned by the sequential approach *(Scenario C2)*, with the difference in variability cost providing most of the cost savings. The computational time required by the integrated approach is approximately six times higher than that of the sequential approach, due to the increased complexity of the integrated problem, which grows in size with every iteration due to an expanding critical set. In the final iteration of the proposed approach, the flexibility problem consisted of 81,228 equations and 76,451 variables, while the sequential problem included 29,218 equations and 27,641 variables. As shown in Table 7, the integrated approach has a 14 % higher capital cost, and a six-fold increase in transition cost. These differences in design and scheduling result in much better performance of the system, reducing variability cost by 69 %. Since variability cost has the largest impact, this results in a lower overall cost for the integrated method, suggesting that integration allows for better balancing between decisions, as they are made simultaneously. Note that the production sequence is completely different, aside from the first point (which is fixed). The transition times are also slightly different, with the integrated approach having a longer first transition. This suggests that scheduling is influenced by design and control decisions, indicating the need for integration of design, control, and scheduling.

Table 7: Summary of Results from Scenario C

Method	*Integrated approach (Scenario C1)*	*Sequential approach (Scenario C2)*
Optimal Process Cost ($)	1,612	2,963
Capital Cost ($)	227	200
Transition Cost ($)	302	50
Variability Cost ($)	1,083	2,713
CPU Time (s)	5,836 (3 iterations)	1,079 (sum of all stages)
Reactor Length L (m)	22.7	20.0 (backed off from 30)
Controller K_c, τ_i	0.1, 100	0.1, 100
Production sequence	E-D-C-A-B	E-C-A-B-D
Transition times Δt (s)	261, 10, 10, 11, 10	10, 10, 10, 10, 10

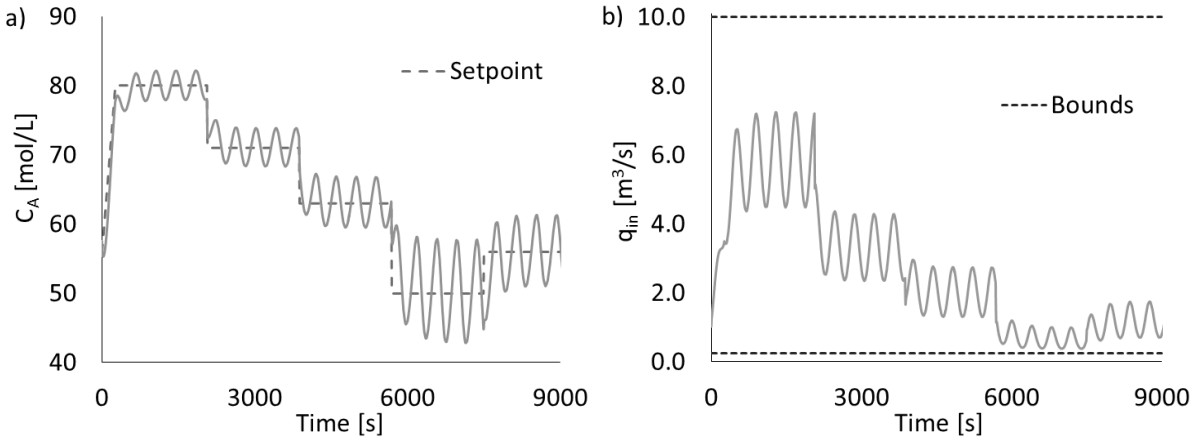

Figure 11: (a) Profiles of outlet concentration and (b) inlet flow rate from Scenario C1

The response in outlet concentration C_A due to the most critical realization in the integrated approach *(Scenario C1)* is shown in Figure 11. As shown in Figure 11a, the concentration follows the set-point, though the oscillatory effect of the disturbance is significant. Note that the first transition duration is longer to accommodate the large change in set-point. In Figure 11b, the manipulated variable (q_{in}) continuously oscillates in *Scenario C1* to partially counteract the disturbance and uncertainty effects, and remains within its bounds at all times.

3.8 Chapter Summary

The critical set method offers a solution for design, control, and scheduling, subject to a discrete set of disturbance and uncertainty. The algorithm identifies infeasible realizations in the feasibility analysis, and assembles a critical set of realizations, which are optimized in the flexibility problem. This method is shown to provide high quality solutions for both a CSTR and PFR case study. These solutions require higher computational time than the sequential method, but offer reduced process cost.

The performance of the critical set method is heavily influenced by the choice of the discrete realizations for the disturbance and uncertainty. As most real random variables have a continuous distribution, the discrete realizations are merely an approximation. A coarse discretization will lose too much information, as nothing between the points is considered, and the result may not be feasible once subjected to the real disturbance and uncertainty. On the other hand, a very fine discretization is not a good choice either. This will cause problems with termination of the algorithm, as the critical set will likely be very large before it converges. Recall that as the critical set grows, the problem size increases, leading to very large problems in this case that may take prohibitively long to solve. Therefore, the discretization must be chosen carefully to allow the critical set method to run properly.

This provides motivation for a method that does not require discretization of disturbance and uncertainty, and instead uses a probabilistic distribution. Such a method would avoid the problem of choosing a suitable discretization, and would allow the use of statistical methods in determining the process variability. The back-off method accomplishes this, and it is described in the next section.

Chapter 4: Back-Off Methodology

This section describes the second method that is utilized in this thesis, the back-off method. This method considers probabilistic distributions for the disturbance and uncertainty. The variability is propagated through the process model using simulations, providing statistical information on all process variables. Back-off terms are generated from this information, and are incorporated into the optimization to back off from the solution at nominal conditions. To reduce conservatism in the solution, this method can be tuned to accommodate different levels of variability. This work presented in this section has been submitted to the AIChE Journal.

The back-off method described in this section is adapted from Shi et al. (2016). The problem definition is the same as in Section 3.1. The formal optimization formulation (29) is presented for a problem without disturbance or uncertainty (referred to as the nominal optimization problem). The required modifications for a stochastic optimization (subject to stochastic realizations in the disturbance and uncertainty) are explained next, including description of back-off terms, followed by the presentation of the back-off algorithm.

Problem (29) presents the deterministic formulation for integration of design, scheduling, and control. Decisions are made on design, control, and scheduling to minimize the total cost of the process, z. The design decisions $\boldsymbol{\mathcal{D}}$ represent process design variables (e.g. equipment sizing, number of distillation trays) and steady-state operating conditions. The control decisions $\boldsymbol{\mathcal{C}}$ represent the process controller tuning, e.g. K_c and τ_i in the case of a PI controller, or control actions in the case of optimal open-loop control. The scheduling decisions represent the production sequence $\boldsymbol{\mathcal{S}}$ (a binary matrix that determines the sequence of production), and the duration $\boldsymbol{\Delta t}$ of each transition between operating points. Note that the transition durations $\boldsymbol{\Delta t}$ are explicitly obtained from optimization, and do not depend on process dynamics, as described in our previous work (Koller and Ricardez-Sandoval, 2017a). For

simplicity, all these variables are referred to as the decision variables $\boldsymbol{\mathcal{E}} = \{\boldsymbol{\mathcal{D}}, \boldsymbol{\mathcal{C}}, \boldsymbol{\mathcal{S}}, \boldsymbol{\Delta t}\}$, and they are limited by upper and lower bounds.

$$\min_{\boldsymbol{\mathcal{E}}=\{\boldsymbol{\mathcal{D}},\boldsymbol{\mathcal{C}},\boldsymbol{\mathcal{S}},\boldsymbol{\Delta t}\}} z\left(\boldsymbol{x}(t), \boldsymbol{u}(t), \boldsymbol{y}(t), \boldsymbol{y}^{sp}(t), \bar{\boldsymbol{d}}(t), \bar{\boldsymbol{p}}, \boldsymbol{\mathcal{D}}, \boldsymbol{\mathcal{C}}, \boldsymbol{\mathcal{S}}, \boldsymbol{\Delta t}\right) \tag{29}$$

$s.t.$

$$\boldsymbol{f}\left(\boldsymbol{x}(t), \dot{\boldsymbol{x}}(t), \boldsymbol{u}(t), \boldsymbol{y}(t), \boldsymbol{y}^{sp}(t), \bar{\boldsymbol{d}}(t), \bar{\boldsymbol{p}}, \boldsymbol{\mathcal{D}}, \boldsymbol{\mathcal{C}}, \boldsymbol{\mathcal{S}}, \boldsymbol{\Delta t}\right) = \boldsymbol{0}$$

$$\boldsymbol{g}\left(\boldsymbol{x}(t), \boldsymbol{u}(t), \boldsymbol{y}(t), \boldsymbol{y}^{sp}(t), \bar{\boldsymbol{d}}(t), \bar{\boldsymbol{p}}, \boldsymbol{\mathcal{D}}, \boldsymbol{\mathcal{C}}, \boldsymbol{\mathcal{S}}, \boldsymbol{\Delta t}\right) \leq \boldsymbol{0}$$

$$\boldsymbol{h}\left(\boldsymbol{x}(t), \boldsymbol{u}(t), \boldsymbol{y}(t), \boldsymbol{y}^{sp}(t), \bar{\boldsymbol{d}}(t), \bar{\boldsymbol{p}}, \boldsymbol{\mathcal{D}}, \boldsymbol{\mathcal{C}}, \boldsymbol{\mathcal{S}}, \boldsymbol{\Delta t}\right) = \boldsymbol{0}$$

$$\boldsymbol{\mathcal{E}}_{lo} \leq \boldsymbol{\mathcal{E}} \leq \boldsymbol{\mathcal{E}}_{up}$$

$$\boldsymbol{\mathcal{S}} \in \{0,1\}$$

$$t \in [0, t_{end}]$$

The notation is the same as in Problem (1), but the difference is that the process disturbances $\bar{\boldsymbol{d}}(t)$ and uncertain parameters $\bar{\boldsymbol{p}}$ are assumed to be at their nominal values. A solution for (29) can be obtained, given that disturbance and/or uncertainty effects are set to their nominal values. If the process disturbances and uncertain parameters are considered as randomly distributed variables, the problem becomes much more difficult to solve, as an infinite search space must be explored to optimize every possible random realization in these variables. The problem then becomes an infinite-dimensional mixed integer non-linear dynamic optimization problem, which is very challenging to solve, due to the aforementioned infinite search space, the solution of time-dependent differential equations, and the combination of binary (sequencing) and continuous decisions. The proposed back-off method explained in the next section attempts to overcome these difficulties, by "backing off" from the solution of the nominal optimization problem (29).

4.1 Back-Off Parameters

The back-off method described in this section has been adapted from that presented in Shi et al. (2016). This section describes the theory of back-off terms, while the calculation and implementation of the back-off terms are discussed in the following section. Consider the set of the inequality constraints $\boldsymbol{g}$ in Problem (29). Subject to stochastic parameter uncertainty $\boldsymbol{p}$ and process disturbances $\boldsymbol{d}$, the constraints cannot be guaranteed to be satisfied by every realization, especially when considering an unbounded distribution such as a normal distribution. Thus, back-off terms $\boldsymbol{b}$ are introduced to each inequality constraint $\boldsymbol{g}$ to approximate the effect of uncertainty, and force the solution to back off from the optimal nominal solution. If a single back-off value is used for all time points, the solution will be very conservative, as the maximum variability will be considered for the entire time domain. In the present analysis, the back-off terms $\boldsymbol{b}(t)$ will be dependent on time, to allow for less conservatism in the solution. Thus, back-off terms will exist for each constraint at each point in time t. Using the described back-off method, the resulting solution can accommodate a specified multiple of standard deviation in the constraints, which is related to the magnitude of the back-off.

The back-off terms are calculated from the results of Monte Carlo simulations, where the levels of the decision variables $\boldsymbol{\mathcal{E}}$ are fixed. However, the back-off terms may depend on the decision variables (i.e. different back-off terms are required for feasibility if design parameters are adjusted). To account for this, the back-off parameters can be identified as functions of the decision variables, via a sensitivity analysis, to generate PSE approximations. A similar approach can be used to generate a PSE for the objective function, to represent how the decision variables affect the process economics under uncertainty. This PSE-based method has shown to be useful for integration of design and control (Mehta and Ricardez-Sandoval, 2016; Rafiei-Shishavan et al., 2017a); alternatively, adjoint sensitivities can be employed (Diehl et al., 2006). However, both of these methods may be very expensive, especially for large-scale applications (Shi et al., 2016). To simplify the present analysis, the effect of uncertainty is assumed to be insensitive to the decision variables, as shown in (30) and (31). To circumvent this issue,

we propose an iterative approach that updates the back-off terms through Monte Carlo simulations for fixed values of the decision variables $\boldsymbol{\mathcal{E}}$, obtained from optimization (see next section). When the assumptions in conditions (30) and (31) do not hold, optimal back-off solutions cannot be guaranteed. Nevertheless, the proposed iterative approach gradually improves the back-off terms $\boldsymbol{b}(t)$ and therefore the solution in the decision variables $\boldsymbol{\mathcal{E}}$. Moreover, the back-off approach is closely related to multi-scenario optimization, which directly incorporates uncertainty. In the multi-scenario approach, the probability distribution of the uncertain parameters is represented by a finite (discrete) set of scenarios, each with a particular probability of occurrence (i.e. weight). Provided that first-order KKT optimality conditions for the multi-scenario optimization hold and critical realizations in the uncertain parameter set are active at the solution, Shi et al. (2016) showed that the present back-off calculation is equivalent to the multi-scenario problem, as long as assumptions (30) and (31) are satisfied.

$$\nabla_{\mathcal{E}} \boldsymbol{b}(t, \boldsymbol{d}, \boldsymbol{p}, \boldsymbol{\mathcal{E}}) \approx 0 \tag{30}$$

$$\nabla_{\mathcal{E}} z(\boldsymbol{d}, \boldsymbol{p}, \boldsymbol{\mathcal{E}}) - \nabla_{\mathcal{E}} z\left(\bar{\boldsymbol{d}}, \bar{\boldsymbol{p}}, \boldsymbol{\mathcal{E}}\right) \approx 0 \tag{31}$$

4.2 Algorithm Formulation

This section discusses the steps that are necessary to generate a robust solution using the back-off method. In the present analysis, the time domain is discretized in the same manner as described in Section 3.3, into regions i, finite elements j, and collocation points k. Similarly, the duration Δt_i of each region i is a decision variable, determined from the optimization, and the duration of the contained finite elements and collocation points will stretch/compress to fit in each region.

The back-off optimization formulation is shown in (32), including back-off terms and time discretization. During the optimization, the back-off terms remain fixed, and are recalculated in each iteration of the algorithm, using MC simulations. Note that uncertainty and disturbances are at their nominal values in Problem (32); however, process variability is approximated by the time-dependent back-off terms. Due to

this approximation, an iterative approach must be taken, where the back-off terms are updated in every iteration. As such, Problem (32) must be solved over multiple iterations in the back-off algorithm until convergence is achieved. The flowchart for the proposed back-off algorithm for integration of design, scheduling and control is shown in Fig. 12. Each of the steps in the algorithm is explained in detail below.

$$\min_{\boldsymbol{\mathcal{E}}=\{\boldsymbol{\mathcal{D}},\boldsymbol{\mathcal{C}},\boldsymbol{\mathcal{S}},\boldsymbol{\Delta t}\}} z\left(\boldsymbol{x}_{ijk},\boldsymbol{u}_{ijk},\boldsymbol{y}_{ijk},\boldsymbol{y}^{sp}_{ijk},\overline{\boldsymbol{d}}_{ijk},\overline{\boldsymbol{p}},\boldsymbol{\mathcal{D}},\boldsymbol{\mathcal{C}},\boldsymbol{\mathcal{S}},\boldsymbol{\Delta t}\right) \tag{32}$$

$s.t.$

$$\sum_{k'} \mathcal{A}_{kk'} x_{ijk'} = \delta t_i \, \boldsymbol{f}\left(\boldsymbol{x}_{ijk},\boldsymbol{u}_{ijk},\boldsymbol{y}_{ijk},\boldsymbol{y}^{sp}_{ijk},\overline{\boldsymbol{d}}_{ijk},\overline{\boldsymbol{p}},\boldsymbol{\mathcal{D}},\boldsymbol{\mathcal{C}},\boldsymbol{\mathcal{S}},\Delta t_i\right), \quad \forall i,j,k$$

$$\boldsymbol{g}\left(\boldsymbol{x}_{ijk},\boldsymbol{u}_{ijk},\boldsymbol{y}_{ijk},\boldsymbol{y}^{sp}_{ijk},\overline{\boldsymbol{d}}_{ijk},\overline{\boldsymbol{p}},\boldsymbol{\mathcal{D}},\boldsymbol{\mathcal{C}},\boldsymbol{\mathcal{S}},\Delta t_i\right) + b_{ijk} \leq 0\,, \quad \forall i,j,k$$

$$\boldsymbol{h}\left(\boldsymbol{x}_{ijk},\boldsymbol{u}_{ijk},\boldsymbol{y}_{ijk},\boldsymbol{y}^{sp}_{ijk},\overline{\boldsymbol{d}}_{ijk},\overline{\boldsymbol{p}},\boldsymbol{\mathcal{D}},\boldsymbol{\mathcal{C}},\boldsymbol{\mathcal{S}},\Delta t_i\right) = 0\,, \quad \forall i,j,k$$

$$\boldsymbol{\mathcal{E}}_{lo} \leq \boldsymbol{\mathcal{E}} \leq \boldsymbol{\mathcal{E}}_{up}$$

$$\boldsymbol{\mathcal{S}} \in \{0,1\}$$

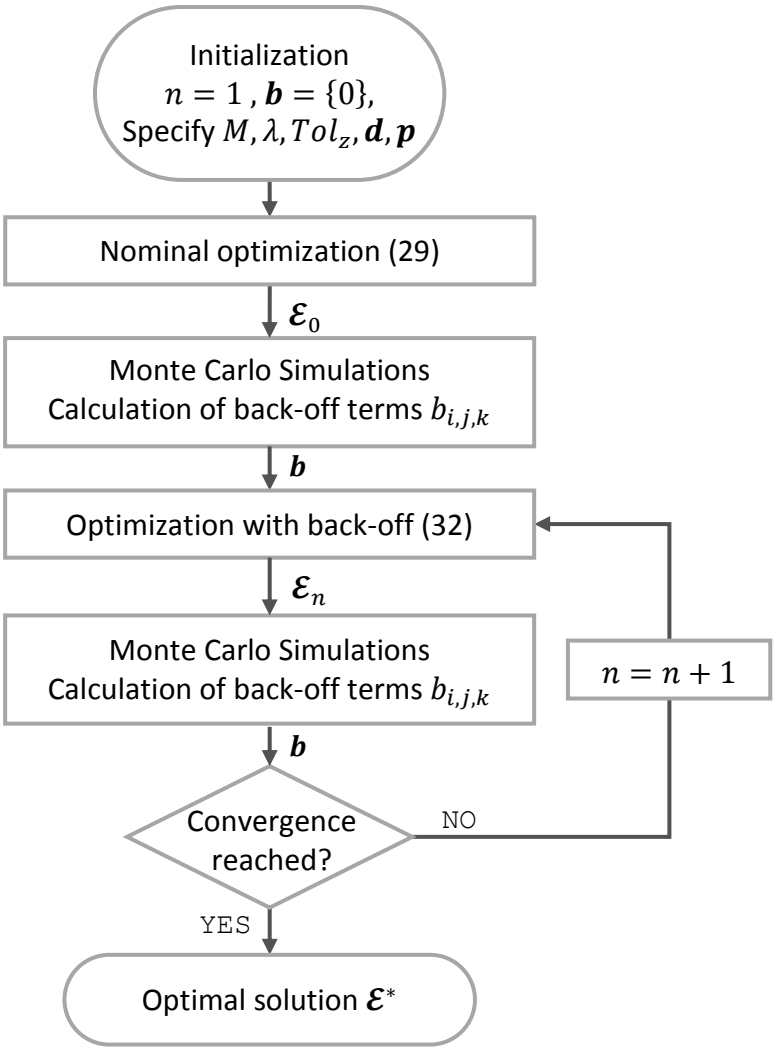

Figure 12: Back-Off Algorithm Flowchart

Step 0: Initialization. Set all the back-off terms $\boldsymbol{b}$ to 0, set the algorithm iteration number n to 1; also, specify the number of MC simulations M, the back-off multiplier λ, the convergence tolerance criteria Tol_z, and define the probability distributions for the uncertain parameters $\boldsymbol{p}$ and process disturbances $\boldsymbol{d}$.

Step 1: Nominal Optimization. The optimization problem (29) using nominal conditions for the uncertain and disturbance variables is solved first, i.e. $\overline{\boldsymbol{d}}(t)$ and $\overline{\boldsymbol{p}}$. For this step, back-off terms are considered to be zero, as defined in the initialization. The optimal (nominal) solution provides a starting point for the algorithm. As shown in Fig. 12, the levels of the decision variables $\boldsymbol{\mathcal{E}}_0$ from this solution are passed to Step 2.

Step 2: Calculate back-off terms via Monte Carlo sampling. Using the known probability distribution for the uncertain parameters $\boldsymbol{p}$ and process disturbances $\boldsymbol{d}$, MC realizations for the uncertain parameters and disturbance sets are generated using the MC sampling technique. For each sampled realization, the system is simulated, and the process response at each discrete point in time is recorded. Note that in the simulations, the decision variables $\boldsymbol{\mathcal{E}}$ are fixed from either the nominal optimization problem (29) (in the first iteration) or the back-off optimization problem (32) (in further iterations), as shown in Fig. 12. These simulations are relatively fast due to the fact that it is a constrained problem, not an optimization.

As shown in (33), the back-off terms $b_{i,j,k}$ for each constraint $g_{i,j,k}$ are equal to a multiple λ of the standard deviation $\sigma_{M,i,j,k}$ for that constraint, at each point in time (i,j,k), after M MC simulations. The way to compute $b_{i,j,k}$ is as follows: after the results from each MC simulation (i.e. referred to as m) are obtained, the mean $\mu_{m,i,j,k}$ and standard deviation $\sigma_{m,i,j,k}$ of each process constraint are calculated, as shown in (34) and (35). This calculation is used to update the mean and variance and is performed after each sample m, to avoid storing all the values from every realization, which would require large amounts of computer memory (i.e. every constraint in every MC sample m at every point in time (i,j,k)). Thus, the subscript m indicates that the statistical parameters have been calculated based on m realizations. The total number of MC samples M used to simulate the system is chosen to be sufficiently large, so that the population of samples is properly representative of the distribution function and adequately captures the system variability for a fixed design, control and scheduling scheme ($\boldsymbol{\mathcal{E}}$). Alternatively, convergence in the statistical parameters (i.e. mean and variance of the process constraints) can also be achieved by embedding the MC simulations within a batch comparison loop. Batches of MC samples are generated and simulated, and then statistical parameters are calculated and compared to the previous batch. New batches are produced until the difference in parameters between successive batches falls below a user-defined tolerance criterion.

$$b_{i,j,k} = \lambda \sigma_{M,i,j,k}; \quad \forall i,j,k \tag{33}$$

$$\mu_{m,i,j,k} = \frac{(m-1)\cdot \mu_{m-1,i,j,k} + g_{i,j,k}}{m}; \quad \forall m,i,j,k \tag{34}$$

$$\sigma^2_{m,i,j,k} = \frac{m-2}{m-1}\cdot \sigma^2_{m-1,i,j,k} + \frac{\left(g_{i,j,k} - \mu_{m-1,i,j,k}\right)^2}{m}; \quad \forall m,i,j,k \tag{35}$$

Step 3: Back-off optimization. The optimization problem (32) is solved with consideration of back-off terms obtained from Step 2. This results in a more conservative solution than that obtained from Step 1, though the updated solution takes into account process variability due to uncertainty and disturbance effects in the process. Note that within the optimization problem (32), only nominal values are considered for parameter uncertainty and process disturbance, while the back-off terms provide information about the stochastic nature of those variables, and their effect on the process. Once a solution is obtained, the levels of the decision variables are passed back to Step 4 to calculate new back-off terms, as shown in Fig. 12.

Step 4: Calculate back-off terms via Monte Carlo sampling. The back-off terms from MC simulations are calculated in this step. This procedure is identical to that described in Step 2, but the fixed decision variables that are provided to this method are from the back-off optimization (Step 3), i.e. ($\boldsymbol{\mathcal{E}}_n$) as opposed to the nominal optimization problem (29), as outlined in Step 1.

Step 5: Algorithm convergence. In each iteration m of the back-off algorithm, an expected objective function value $E[z]_n$ is calculated, to evaluate the average quality of the solutions from the MC simulations in that iteration. If this expected objective value is within a specified tolerance Tol_z of the previous iteration (i.e. if condition (36) is true), and if there are no expected constraint violations (i.e. $\Gamma \leq 0$ in (37)), then terminate the algorithm, and return the current solution $\boldsymbol{\mathcal{E}}_n$ as the optimal design, control and scheduling scheme. If either of the convergence criteria do not hold, the algorithm returns to Step 3. As shown in (38), the inequality constraints $\boldsymbol{g}$ are instead evaluated using statistical parameters (i.e. mean and back-off), which are generated after M MC stochastic realizations in the disturbances and uncertain parameters, using the current design, control and schedule scheme ($\mathcal{E}_n$). Note that the mean values and the back-off terms are evaluated at each time point i,j,k, and the largest constraint violation is recorded

as Γ, as shown in (37). A positive value in Γ indicates a constraint violation, i.e. the current design, control and scheduling solution ($\mathcal{E}_n$) is dynamically infeasible. Note that this is not the worst case among M realizations from the MC simulations, but the worst case *in time*, based on the mean value of each constraint $\boldsymbol{g}$ plus λ standard deviations.

$$\frac{|E[z]_n - E[z]_{n-1}|}{E[z]_n} \leq Tol_z \tag{36}$$

$$\Gamma = \max_{i,j,k}\left(\mu_{M,i,j,k} + b_{i,j,k}\right) \tag{37}$$

$$\boldsymbol{g}\left(\boldsymbol{x}_{i,j,k}, \boldsymbol{u}_{i,j,k}, \boldsymbol{y}_{i,j,k}, \boldsymbol{y}^{sp}_{i,j,k}, \boldsymbol{d}_{i,j,k}, \boldsymbol{p}, \boldsymbol{\mathcal{E}}\right) \leq 0 \leftrightarrow \left(\mu_{M,i,j,k} + b_{i,j,k}\right) \leq 0 \quad \forall i,j,k \tag{38}$$

As stated previously, a limitation of this method is that large back-off terms will shrink the feasible region, so that finding a solution may be more difficult. This can lead to convergence failure, particularly if few degrees of freedom are able to adapt to uncertainty. In addition, highly non-linear and highly coupled problems may cause issues due to local optima in the optimization step, and invalid assumptions (30) and (31) of back-off terms. Furthermore, the algorithm may not always produce the same result every time, due to the random nature of the MC simulations considered in the proposed back-off algorithm. Despite these limitations, the algorithm has been effective in previous case studies (Shi et al., 2016).

4.3 Application of Back-off Methodology to Non-Isothermal CSTR

The Back-Off Method is applied to the same CSTR case study as in Section 3.6. The case study will not be described in this section, aside from the modifications made. The uncertain parameters are changed to a normal distribution, as defined in (39) and (40). To provide a similar level of uncertainty, the mean value plus/minus two sigma is set to the bounds of the discrete realizations from Section 3.6. The same time discretization is used, except the duration of the production regions has been shortened to 360 s, and the minimum transition time from Eq. (20) has been reduced to 5 s.

$$E_R \sim \mathcal{N}(20000, 500^2) \tag{39}$$

$$\Delta H_R \sim \mathcal{N}(5000, 500^2) \tag{40}$$

The back-off algorithm presented in the previous section was implemented on this multi-product case study. The results presented in the next sections were obtained using a system running Windows 7, using an Intel® Core™ i7-2600 CPU 3.40 GHz and 8.00 GB RAM. The back-off method for this case study was implemented in GAMS (Brooke et al., 2007). For each NLP, CONOPT (Drud, 1985) is the selected solver, and locally optimal solutions are accepted due to the non-linear nature of the problem. For the MC simulations, an explicit time-stepping method is used to simulate the system at each realization of uncertainty and disturbance. The flexibility problems (29) and (32) described in the back-off algorithm presented in this work are MINLP due to the scheduling decisions. However, if only a few binary variables are present, it is straightforward to enumerate all the possible sequences and solve non-linear programs (NLPs) for each case. This was done in the present case study. To simplify the analysis, the first product in the sequence is set to grade A, reducing the search space to 24 sequences.

4.3.1 Scenario D: PI Control with Different Back-off Levels

This scenario is named *Scenario D*, following the naming scheme of the previous scenarios, and to avoid confusion with *Scenario A.* In the current scenario, solutions are generated for multiple values of the back-off multiplier λ, which consist of 0 (no back-off) and then 1, 2, and 3 (increasing levels of back-off). The process is controlled by a PI controller as in (41), defined by the proportional gain K_c and the integral time τ_i, to control the product concentration C_B at the outlet by manipulating the heating rate Q_H. Recall, that the process disturbance is the inlet flow rate q_{in}, which oscillates a frequency ω. For this scenario, the disturbance frequency ω is assumed to be fixed at $0.08\ rad/s$. Note that this describes a constant oscillation frequency ω, not a constant value for q_{in}.

$$Q_H(t) = \overline{Q_H} + K_C\left(C_B^{sp} - C_B(t)\right) + \frac{K_c}{\tau_i}\int_0^t \left(C_B^{sp} - C_B(t')\right) dt' \quad (41)$$

For *Scenario D*, only uncertainty in the activation energy E_R and heat of reaction ΔH_R was considered. The number of MC simulations M is set to 20,000, and the algorithm convergence tolerance Tol_z is set to 1%. These values were found to be sufficient in preliminary analysis.

The results from each of the four scenarios are displayed in Table 8. The average process cost z_{CSTR} is calculated from the MC simulations in each scenario, considering λ standard deviations of variability in the output concentration (which affects process cost) as well as reactor temperature and heat input (which affect dynamic feasibility).

Table 8: Summary of Results from Scenario D and Scenario E

Scenario	*Scenario D0*	*Scenario D1*	*Scenario D2*	*Scenario D3*	*Scenario E*
Back-off multiplier λ	0	1	2	3	2
Disturbance q_{in}	Nominal ω	Nominal ω	Nominal ω	Nominal ω	Stochastic ω
Average process cost z_{CSTR}	445	503	576	675	588
CPU time (s)	2.18×10^3	40.9×10^3	70.7×10^3	28.8×10^3	72.9×10^3
Reactor Volume $V(L)$	16.1	17.4	19.1	21.4	19.0
Controller K_C, τ_i	5.00, 244	5.00, 325	5.00, 1000	5.00, 1000	5.00, 652
Production sequence	A-B-D-E-C	A-C-E-B-D	A-E-B-C-D	A-E-B-C-D	A-C-E-B-D
Transition times $\boldsymbol{\Delta t}$ (s)	23.3, 8.4, 20.0, 16.0, 43.7	30.1, 44.1, 40.5, 17.2, 18.3	31.4, 41.4, 28.8, 40.9, 49.1	32.1, 38.4, 32.7, 41.0, 47.2	31.5, 35.2, 47.1, 17.0, 19.0

As shown in Table 8, *Scenario D0* represents the case where no uncertainty or back-off parameters are considered in the analysis, i.e. ($\lambda = 0$). Accordingly, this scenario produces the most economically attractive solution; however, the design, control and scheduling scheme obtained from this scenario becomes infeasible when subjected to uncertainty. The subsequent solutions show increasing levels of robustness, where *Scenarios D1, D2,* and *D3* can withstand one, two, and three standard deviations of process variability, respectively. This robustness comes at a cost, however, as the average total process cost increases. This is because the system must back-off from the nominally optimal solution to ensure feasibility under stochastic realizations in the uncertain parameters. Furthermore, the

computational complexity is greatly increased, as scenarios beyond *Scenario D0* show at least an order of magnitude increase in computational costs. Due to the random and non-linear nature of the problem, there is not a direct correlation, as *Scenario D3* exhibited a lower computational time than *Scenario D2*. The reactor volume can be seen to increase as the back-off multiplier increases, so that the increased volume acts as a buffer to reduce variability. Longer transition times can also be seen in cases with higher back-off, as this allows the system more time to transition to the next operating point, reducing variability. Controller parameters do not change significantly, though the integral action becomes slightly slower as more back-off is considered. Three different production sequences can be seen among the five scenarios shown in Table 8, indicating that scheduling decisions can have a significant effect on process dynamics, and can be influenced by design and control decisions.

Output concentration for *Scenario D1* and *Scenario D2* is shown in Fig. 13, where the difference in production sequence can be observed. Both scenarios show similar set-point tracking, oscillating around the set-point due to the process disturbance. Confidence regions for concentration are shown in Fig. 13, but they are almost negligible due to effective feedback controller actions. Reactor temperature for *Scenario D2* is shown in Fig. 14, where the confidence region can be clearly observed. This indicates that the PI controller is effective at removing variability from the concentration and transferring it to the temperature. Note that the upper confidence bound on temperature just touches the operating limit, indicating that it is a binding constraint, and that the back-off algorithm terminated properly.

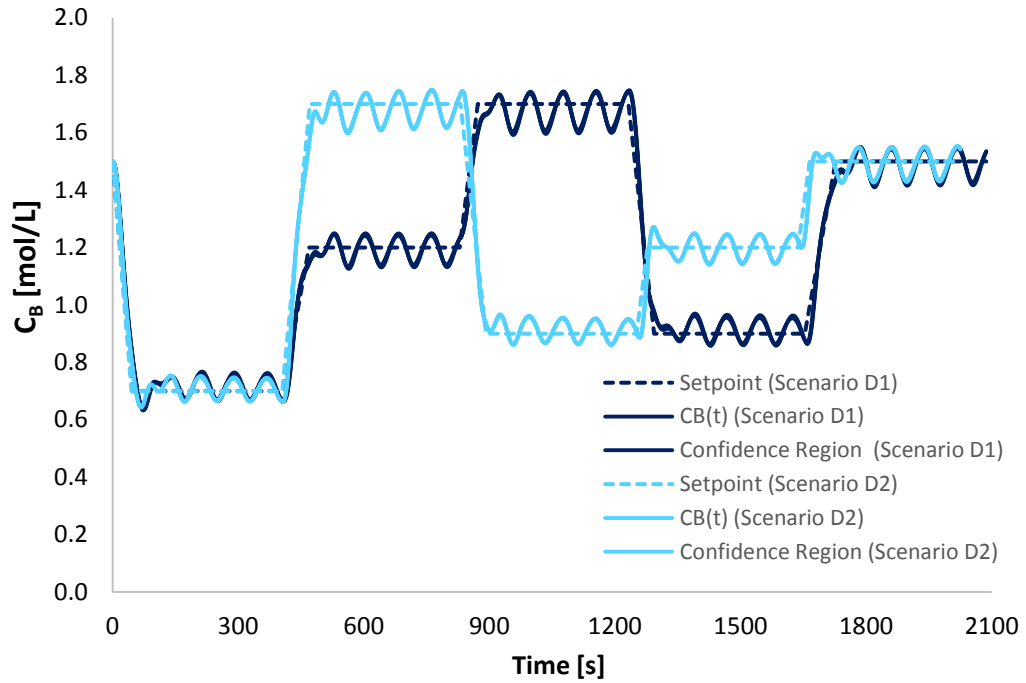

Figure 13: Plot of output concentration for Scenario D1 and Scenario D2

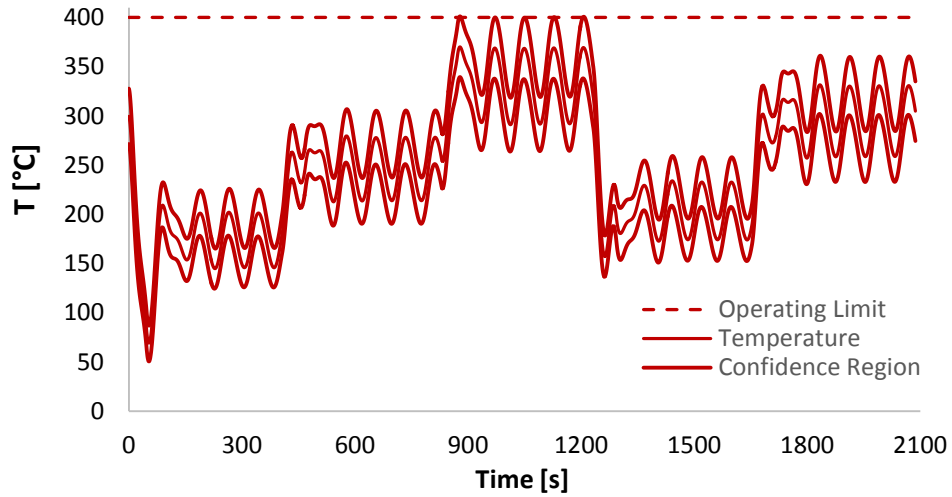

Figure 14: Plot of reactor temperature for Scenario D2

4.3.2 Scenario E: PI Control with Stochastic Process Disturbance

This scenario investigates the effect of a stochastic process disturbance. In the previous scenario, uncertainty in the activation energy E_R and heat of reaction ΔH_R were considered in the analysis. This scenario extends *Scenario D* and considers uncertainty in the process disturbance q_{in}, the inlet flow rate

to the reactor. For this scenario, the oscillation frequency ω will be a stochastic variable, distributed as in (42). The original two uncertain parameters (i.e. E_R and ΔH_R) are also considered in this scenario. The back-off multiplier λ is set to 2 standard deviations for this scenario. The algorithm convergence tolerance is the same as in *Scenario D*. Due to the addition of a time-dependent stochastic variable (the process disturbance), the total number of MC simulations M has been increased to 100,000 to ensure convergence of the statistical parameters (mean and back-off) for each constraint.

$$\omega \sim \mathcal{N}(0.08, 0.0008^2) \tag{42}$$

Results from *Scenario E* are shown in Table 8. *Scenario E* shows a similar solution to *Scenario D2*, where the average process cost is increased by 2.2% and computational time is increased by 3.2%, due to the consideration of stochastic disturbance. The reactor volume shows no significant change. The controller in *Scenario E* has the same amount of proportional control, but faster integral control. An important result is that the production sequence is different; showing that even minor variability in the process disturbance can affect the optimal production sequence for this process.

Output concentration for *Scenario E* is shown in Fig. 15, where distinct confidence bounds can be observed. This is different from the results obtained for all scenarios in *Scenario D*, where the variability in concentration was almost negligible. This indicates that the stochastic disturbance prevents the controller from transferring all the variability to the temperature; some variability remains with the concentration. Also, the confidence region grows with time, as the variable-frequency sine wave disturbances deviate from one another. Reactor temperature for *Scenario E* is presented in Fig. 16, where the variability is significant, and the operating constraint is binding, similar to the previous scenario.

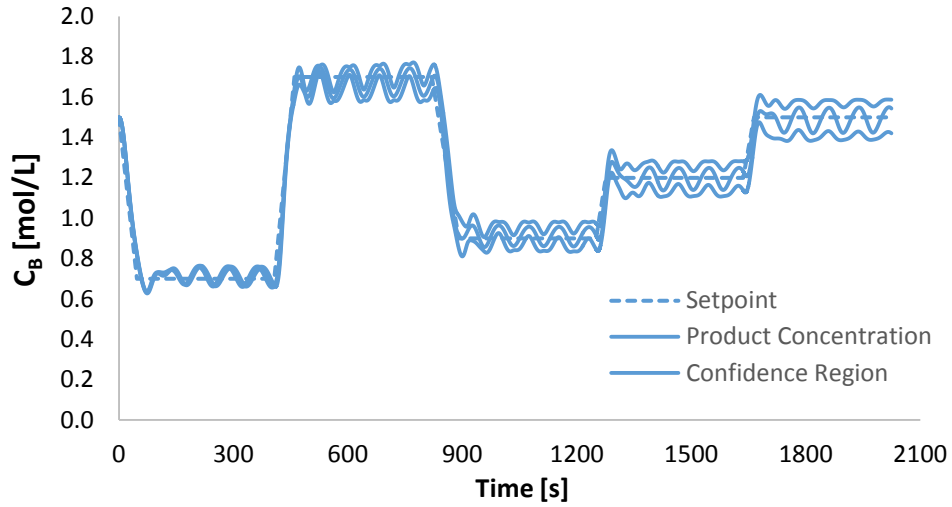

Figure 15: Plot of output concentration for Scenario E

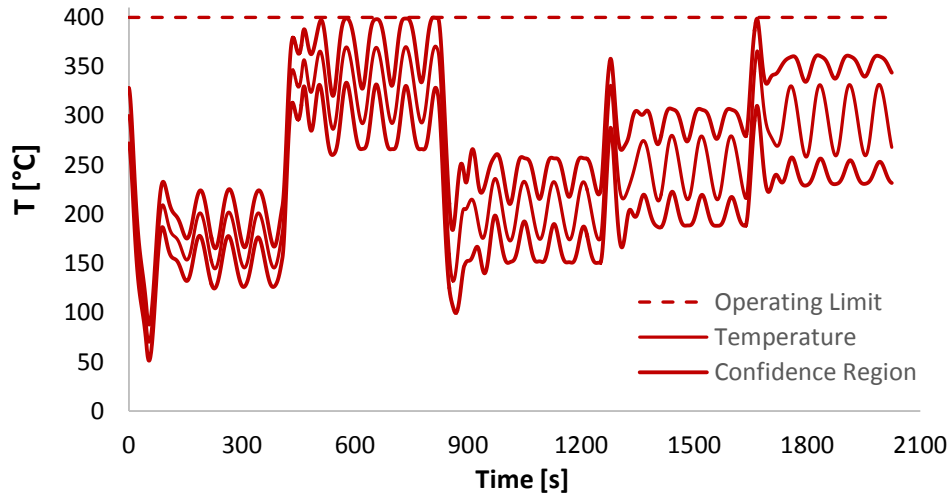

Figure 16: Plot of reactor temperature for Scenario E

4.3.3 Scenario F: Optimal Open-Loop Control

In this scenario, the PI controller is replaced with a manipulated variable profile that is determined directly from dynamic optimization. Therefore, K_c and τ_i are removed from the formulation, and replaced with $(Q_H)_{i,j}$, which represents the heat input, determined at each discretization point specified by the regions (i) and the finite elements (j). To constrain the actions of the controller, additional constraints are placed on the heat input, including upper and lower bounds, as shown in (43),

and rate-of-change limits, as shown in (44). Because the control profile in this scenario is optimized, the nominal case (*Scenario F0*) is expected to offer effective control actions. On the other hand, for operation subject to disturbance or parameter uncertainty, this control profile will remain fixed, likely leading to poor solutions due to the lack of feedback.

The back-off multiplier λ is set to zero and unity for *Scenarios F0* and *F1*, respectively. Nominal disturbance is considered in *Scenarios F0* and *F1*, while stochastic disturbance with the frequency distribution presented in (42) is considered in *Scenario F2*. The algorithm convergence tolerance is the same as in *Scenario D*, and the total number of MC simulations (M) is 20,000 in *Scenarios F0* and *F1*, while it is increased to 100,000 in *Scenario F2* based on the presence of stochastic disturbance.

$$-700\ kW \leq Q_H(t) \leq 1200\ kW \tag{43}$$

$$-10\ \text{kW/s} \leq \frac{dQ_H(t)}{dt} \leq 10\ \text{kW/s} \tag{44}$$

Table 9: Summary of Results from Scenario F

Scenario	*Scenario F0*	*Scenario F1*	*Scenario F2*	*Scenario F3*
Back-off multiplier λ	0	1	1	1
Disturbance q_{in}	Nominal ω	Nominal ω	Stochastic ω	Stochastic ω
Average process cost z_{CSTR}	229	1,104	1,474	1,446
CPU time (s)	2.74×10^3	72.1×10^3	16.0×10^3	54.3×10^3
Reactor Volume $V(L)$	15.0	17.9	17.3	17.2
Production sequence	A-B-C-D-E	A-B-C-D-E	A-D-E-C-B	A-D-E-C-B
Transition times $\boldsymbol{\Delta t}$ (s)	29.6, 5.3, 12.8, 12.3, 8.3	22.0, 3.4, 18.8, 3.5, 21.9	6.8, 16.8, 3.3, 18.0, 13.4	6.9, 17.1, 3.4, 18.4, 13.1

Results from *Scenario F* are shown in Table 9. As expected, *Scenario F0* ($\lambda = 0$) has the lowest cost among all scenarios, but becomes infeasible under uncertainty. *Scenario F1* can accommodate one standard deviation, but pays a very large cost for this ability, as the process cost increases by almost an order of magnitude and the computational time is increased by a factor of 25. This is because the optimal control profile does not change under stochastic operation, as the profile is fixed after it is determined at

each optimization problem (Step 1 or Step 3 of the algorithm). Hence, the dynamic system cannot react as well to uncertainty, resulting in high variability in the output concentration, leading to an increased average process cost. Compared to *Scenario F0*, the reactor volume is 20% larger in *Scenario F1*, which allows the system to help buffer the effect of uncertainty. Transition times are also generally longer, allowing the system more time to reach the next operating point. *Scenario F2* features stochastic disturbance with optimal open-loop control. The average process cost is further increased by 33% with respect to *Scenario F1* as the system has no feedback to control the uncertainty and disturbance. Reactor volume is similar to *Scenario F1*, and transition times are also similar, though in a different order. *Scenario F2* has a different production sequence from the other two scenarios in Table 9, indicating that both stochastic disturbances and parameter uncertainty can affect the optimal production sequence.

Output concentrations for *Scenario F1* and *Scenario F2* are shown in Fig. 17, where the difference in production sequence and process variability can be observed. Due to lack of feedback to the control profile, both scenarios show large confidence bands around the concentration. The profile of the manipulated variable (heat input Q_H) for *Scenario F2* is shown in Fig. 18, where the behaviour of the open-loop controller can be seen oscillating to counteract the process disturbance (recall that the nominal case does include disturbance, though at a known oscillation frequency). The profile does not resemble a sinusoidal wave (to match the disturbance), but a triangle wave, because the rate of change of heat input is limited as per constraint (44). Note that the heat input remains within the operating limits (43) at all times, thus ensuring dynamically feasible operation for this process.

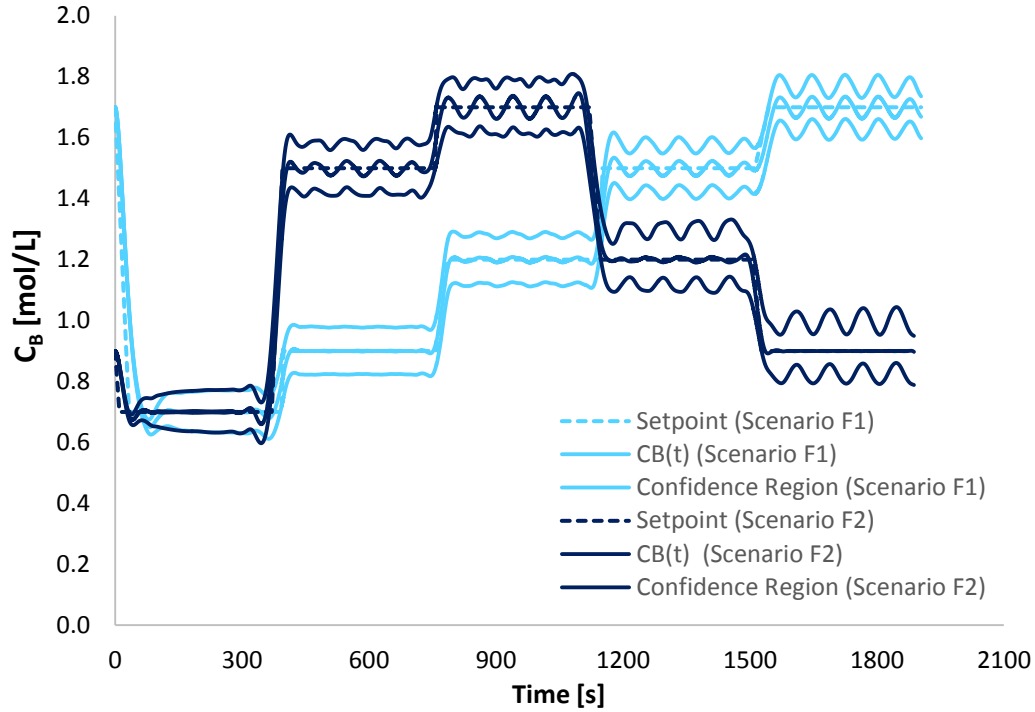

Figure 17: Plot of output concentration for Scenario F1 and Scenario F2

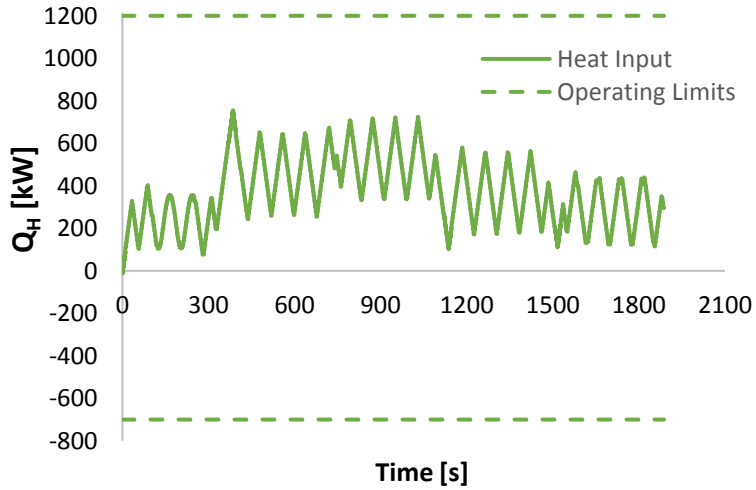

Figure 18: Plot of manipulated variable (heat input) for Scenario F2

To investigate the effect of constraint (19), *Scenario F3* is considered, where the bounds on constraint (44) are relaxed to $\pm$20 kW/s. The results are shown in Table 9, where it can be observed that *Scenario F3* has a slightly lower process cost (-1.9%) than *Scenario F2*, but requires roughly four times the computational effort, partly due to the extra flexibility in the control profile for the heat input Q_H. The decision variables are similar between *Scenario F3* and *Scenario F2*, showing only small differences in

reactor volume and transition durations. As shown in Fig. 19, the product concentration C_B from *Scenario F3* has a very flat profile in the nominal problem, while confidence bands arise from the stochastic MC simulations, due to the lack of controller feedback. As shown in Fig. 20, the heat input has the flexibility to match the disturbance behaviour of a sinusoidal wave, with additional spikes during transition periods.

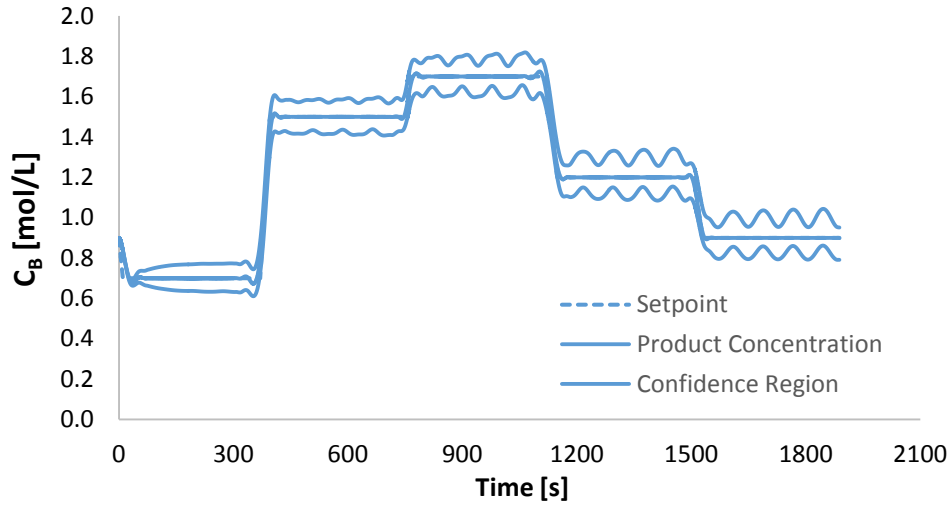

Figure 19: Plot of output concentration for Scenario F3

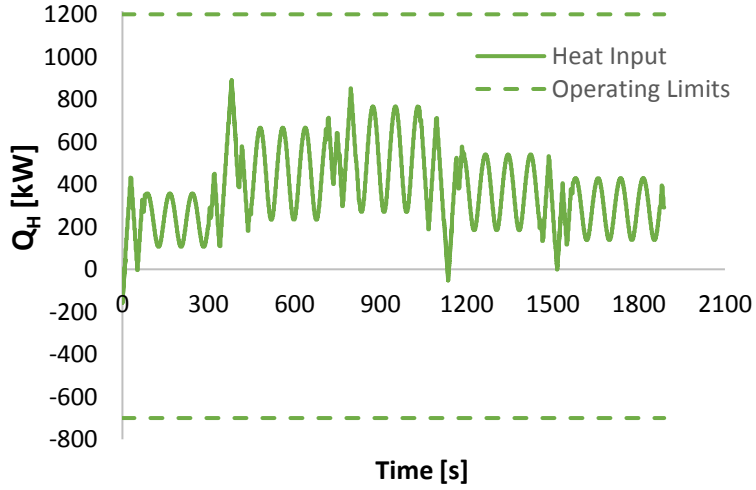

Figure 20: Plot of manipulated variable (heat input) for Scenario F3

4.4 Chapter Summary

The back-off method offers a solution for design, control, and scheduling, subject to stochastic disturbance and uncertainty. The algorithm propagates the probabilistic distributions through the model, from the disturbance and uncertainty input to the process output. Back-off terms are generated from the statistical information, and are incorporated into the flexibility problem to "back off" from the nominal solution. This method is shown to provide high quality solutions for a CSTR case study, using either PI control or open-loop control. These solutions require higher computational time than the nominal optimization, but offer robustness to a specified level of variability.

The performance of the back-off method is heavily influenced by the assumptions made on the probability distributions for the disturbance and uncertainty. In this study, normal distributions were assumed for the process disturbances and parameter uncertainty, because that is a typical distribution for real-world variables. Furthermore, the process output variability was also fitted to a normal distribution, although this may not be a correct assumption for non-linear problems. A more rigorous analysis of the output variability may improve the accuracy of the solution. Regardless, the accuracy of the back-off method is believed to be better than the critical set method due to the lack of discretization for the disturbance and uncertainty. Conclusions and potential improvements on both of these methods are described in the next section.

Chapter 5: Conclusions and Recommendations

5.1 Conclusions

The research developed for this thesis features two algorithms for integration of design, control, and scheduling for multiproduct processes under disturbance and uncertainty. The critical set method is presented, featuring a critical set of realizations, which are incorporated into the flexibility problem. The feasibility analysis determines if there are any infeasible realizations, and then adds those realizations to the critical set. The algorithm provides a solution that is robust to a discrete set of process disturbance and parameter uncertainty. The novelty of this framework is that it performs a direct integration of design, control, and scheduling, while explicitly accounting for scheduling decisions in the process model by the use of variable-sized finite elements in the model discretization. The critical set method was applied to a case study of a multiproduct CSTR. The results from the proposed method are compared to the common alternative, the sequential method. The critical set method is able to return a solution in a practical time frame, with improved feasibility and optimality compared to the sequential method. The critical set method was also applied to a PFR case study, and similar results were observed, offering improved solution quality over the sequential method. This demonstrates applicability of the critical set method to a variety of systems. The results of the critical set method are highly dependent on the discretization of disturbance and uncertainty, so choosing a reasonable discretization scheme can be difficult.

The back-off method is also presented for integration of design, control, and scheduling under stochastic uncertainty and process disturbances. This algorithm combines previous works on integrated optimization and MC based back-off approaches. The key aspect of this algorithm is that it considers stochastic uncertainty and disturbances, using MC sampling and a statistical back-off approach. The algorithm makes decisions on design, control, and scheduling, all of which are incorporated directly into the discretized process model. The solutions produced by this algorithm can accommodate a specified level of variability, while remaining dynamically feasible during operation. The back-off method was

applied to a multiproduct CSTR case study. Considering a system with PI control, the proposed algorithm was able to provide high quality dynamically feasible solutions, with binding constraints indicating that the algorithm ran exactly as expected. For a system with optimal open-loop dynamic control, the algorithm was able to produce dynamically feasible solutions, despite the lack of controller feedback. The constraints were not binding in the solution for the open-loop problem, implying that the back-off parameters were not estimated accurately, and that sensitivity analyses are needed.

Since the methods are applied to the same CSTR case study, the results can be compared between the critical set method (*Scenario B1* in Table 5) and the back-off method (*Scenario D2* in Table 8). The back-off method offers a 5% reduction in total process cost, though at the expense of 17 times the computational effort. The optimal design, control, and scheduling differ slightly between the solutions, likely due to the differences in disturbance and uncertainty. The critical set method may be more desirable in some cases, as it solves much faster, and only provides a slightly worse solution. However, the back-off method may be more generally applicable than the critical set method, as it can accommodate stochastic representations of process disturbance and parameter uncertainty, and the conservatism of the solution can be precisely tuned to a desired level. Therefore, both methods have benefits and limitations; hence, the most suitable method should be chosen based on the computational budget, and the desired quality and robustness of the solution.

Based on the results from the case studies, it is shown that design, control, scheduling, uncertainty, and disturbances can all interact with one another, demonstrating the need for simultaneous optimization. The improvement in solution quality, and the tractable computational time required by the proposed methods show that they could be practical approaches for integrated optimization of design, control, and scheduling.

5.2 Recommendations

The work presented in this thesis can be extend in a number of ways, specifically by changing the assumptions that were made in the development of the proposed methods. These recommendations can provide avenues for further research in the area of integration of design, control, and scheduling.

- Due to the scheduling formulation, these methods are specifically for multiproduct processes. However, they can be extended to consider other processes that require a similar scheduling formulation, e.g. flow-shop systems.
- The methods can be extended to include integer variables in the design and control decision, e.g. number of plates in a distillation column, or selection of a control configuration. This proposed methods only considered integer decisions in the scheduling decisions.
- The methods presented in this thesis can be extended to larger systems to analyze the applicability to large-scale problems, and the scalability of problem complexity.
- The back-off method can be extended to include sensitivity analyses, instead of assuming that the back-off terms are insensitive as in (30) and (31). This can be accomplished using power series expansion (PSE) approximations, relating the back-off parameters to changes in the decision variables. With PSE equations incorporated into the optimization, the back-off parameters would change as the decision variables change, e.g. altering the reactor volume would change the back-off parameters. This would be an improvement over the back-off method presented in this thesis, where the back-off parameters are fixed during the optimization.
- In the back-off method, the process output variability was assumed to follow a normal distribution. Although the stochastic process inputs follow normal distributions, the non-linear nature of the problem may distort the output distribution. Instead of making assumptions about the output distribution, an explicit approach can be used, e.g. taking the 95^{th} percentile of the process output instead of using the calculated mean and variance. This would improve the accuracy of the solution, regardless of the nature of the output distribution.

References

Alvarado-Morales, M., Hamid, M.K.A., Sin, G., Gernaey, K. V., Woodley, J.M., Gani, R., 2010. A model-based methodology for simultaneous design and control of a bioethanol production process. Comput. Chem. Eng. 34, 2043–2061. doi:10.1016/j.compchemeng.2010.07.003

Bahakim, S.S., Ricardez-Sandoval, L.A., 2014. Simultaneous design and MPC-based control for dynamic systems under uncertainty: A stochastic approach. Comput. Chem. Eng. 63, 66–81. doi:10.1016/j.compchemeng.2014.01.002

Bahri, P.A., Romagnoli, J.A., Bandoni, J.A., Barton, G.W., 1995. Back-off Calculations in Optimising Control: A Dynamic Approach 19, 699–708.

Bansal, V., Perkins, J.D., Pistikopoulos, E.N., 2002. A Case Study in Simultaneous Design and Control Using Rigorous, Mixed-Integer Dynamic Optimization Models. Ind. Eng. Chem. Res. 41, 760–778. doi:10.1021/ie010156n

Bhatia, T., Biegler, L., 1996. Dynamic optimization in the design and scheduling of multiproduct batch plants. Ind. Eng. Chem. Res. 5885, 2234–2246. doi:10.1021/ie950701i

Biegler, L.T., 2010. Nonlinear Programming: Concepts, Algorithms, and Applications to Chemical Processes. doi:10.1137/1.9780898719383

Birewar, D.B., Grossmann, I.E., 1989. Incorporating scheduling in the optimal design of multiproduct batch plants. Comput. Chem. Eng. 13, 141–161. doi:10.1016/0098-1354(89)89014-3

Brengel, D.D., Seider, W.D., 1992. Coordinated design and control optimization of nonlinear processes. Comput. Chem. Eng. 16, 861–886. doi:10.1016/0098-1354(92)80038-B

Brooke, A., Kendrick, D., Meeraus, A., Raman, R., Rosenthal, R., 2007. GAMS A User's Guide.

Castro, P.M., Barbosa-Povoa, A.P., Novais, A.Q., 2005. Simultaneous design and scheduling of multipurpose plants using resource task network based continuous-time formulations. Ind. Eng. Chem. Res. 44, 343. doi:10.1021/ie049817h

Chatzidoukas, C., Perkins, J.D., Pistikopoulos, E.N., Kiparissides, C., 2003. Optimal grade transition and selection of closed-loop controllers in a gas-phase olefin polymerization fluidized bed reactor. Chem. Eng. Sci. 58, 3643–3658. doi:10.1016/S0009-2509(03)00223-9

Chu, Y., You, F., 2014a. Model-based integration of control and operations: Overview, challenges, advances, and opportunities. Comput. Chem. Eng. 83, 2–20. doi:10.1016/j.compchemeng.2015.04.011

Chu, Y., You, F., 2014b. Integrated Planning , Scheduling , and Dynamic Optimization for Batch Processes : MINLP Model Formulation and Efficient Solution Methods via Surrogate Modeling. Ind. Eng. Chem. Res. 53, 13391–13411.

Chu, Y., You, F., 2014c. Moving Horizon Approach of Integrating Scheduling and Control for Sequential Batch Processes. AIChE J. 60, 1654–1671. doi:10.1063/1.4866641

Chu, Y., You, F., 2013. Integration of scheduling and dynamic optimization of batch processes under uncertainty: Two-stage stochastic programming approach and enhanced generalized benders decomposition algorithm. Ind. Eng. Chem. Res. 52, 16851–16869. doi:10.1021/ie402621t

Diehl, M., Bock, H.G., Kostina, E., 2006. An approximation technique for robust nonlinear optimization. Math. Program. 230, 213–230. doi:10.1007/s10107-005-0685-1

Drud, A., 1985. CONOPT: A GRG code for large sparse dynamic nonlinear optimization problems. Math. Program. 31, 153–191. doi:10.1007/BF02591747

Engell, S., Harjunkoski, I., 2012. Optimal operation: Scheduling, advanced control and their integration. Comput. Chem. Eng. 47, 121–133. doi:10.1016/j.compchemeng.2012.06.039

Figueroa, J.L., Bahri, P.A., Bandoni, J.A., Romagnoli, J.A., 1996. Economic Impact of Disturbances and Uncertain Parameters in Chemical Processes - A Dynamic Back-off Analysis. Comput. Chem. Eng. 20, 453–461.

Flores-Tlacuahuac, A., Grossmann, I.E., 2011. Simultaneous cyclic scheduling and control of tubular reactors: Parallel production lines. Ind. Eng. Chem. Res. 50, 8086–8096. doi:10.1021/ie101677e

Galvanin, F., I-, M., Dipartimento, D., I-, M., Dipartimento, D., Macchietto, S., 2010. A Backoff Strategy for Model-Based Experiment Design Under Parametric Uncertainty. AIChE J. 56. doi:10.1002/aic.12138

Harjunkoski, I., Nyström, R., Horch, A., 2009. Integration of scheduling and control-Theory or practice? Comput. Chem. Eng. 33, 1909–1918. doi:10.1016/j.compchemeng.2009.06.016

Heo, S., Lee, K., Lee, H., Lee, I., Park, J.H., 2003. A New Algorithm for Cyclic Scheduling and Design of Multipurpose Batch Plants. Am. Chem. Soc. 836–846.

Janak, S.L., Lin, X., Floudas, C.A., 2007. A new robust optimization approach for scheduling under uncertainty. II. Uncertainty with known probability distribution. Comput. Chem. Eng. 31, 171–195. doi:10.1016/j.compchemeng.2006.05.035

Koller, R.W., Ricardez-Sandoval, L.A., 2017a. A Dynamic Optimization Framework for Integration of Design, Control and Scheduling of Multi-product Chemical Processes under Disturbance and Uncertainty. Comput. Chem. Eng. doi:10.1016/j.compchemeng.2017.05.007

Koller, R.W., Ricardez-Sandoval, L.A., 2017b. Integration of Design, Control and Scheduling: A Dynamic Optimization Framework for Multiproduct Chemical Processes under Disturbances and Uncertainty, in: Espuña, A., Graells, M., Puigjaner, L. (Eds.), 27th European Annual Symposium on Computer Aided Chemical Engineering. Elsevier, pp. 2077–2082. doi:http://dx.doi.org/10.1016/B978-0-444-63965-3.50348-2

Kookos, I.K., Perkins, J.D., 2016. Control Structure Selection Based on Economics: Generalization of the Back-Off Methodology. AIChE J. 62, 3056–3064. doi:10.1002/aic.15284

Kookos, I.K., Perkins, J.D., 2001. An Algorithm for Simultaneous Process Design and Control. Ind. Eng. Chem. Res. 40, 4079–4088. doi:10.1021/ie000622t

Lin, X., Floudas, C.A., 2001. Design, synthesis and scheduling of multipurpose batch plants via an effective continuous-time formulation. Comput. Chem. Eng. 25, 665–674. doi:10.1016/S0098-1354(01)00663-9

Luyben, M.L., Floudas, C.A., 1994. Analyzing the interaction of design and control-1. A multiobjective framework and application to binary distillation synthesis. Comput. Chem. Eng. 18, 933–969. doi:10.1016/0098-1354(94)E0013-D

Mansouri, S.S., Sales-Cruz, M., Huusom, J.K., Gani, R., 2016. Systematic integrated process design and control of reactive distillation processes involving multi-elements. Chem. Eng. Res. Des. 115, 348–364. doi:10.1016/j.cherd.2016.07.010

Mehta, S., Ricardez-Sandoval, L. a., 2016. Integration of Design and Control of Dynamic Systems under

Uncertainty: A New Back-Off Approach. Ind. Eng. Chem. Res. 55, 485–498. doi:10.1021/acs.iecr.5b03522

Mendez, C.A., Cerda, J., Grossmann, I.E., Harjunkoski, I., Fahl, M., 2006. State-of-the-art review of optimization methods for short-term scheduling of batch processes. Comput. Chem. Eng. 30, 913–946. doi:10.1016/j.compchemeng.2006.02.008

Mohideen, M.J., Perkins, J.D., Pistikopoulos, E.N., 1996. Optimal design of dynamic systems under uncertainty. AIChE J. 42, 2251–2272. doi:10.1002/aic.690420814

Nie, Y., Biegler, L.T., 2012. Integrated Scheduling and Dynamic Optimization of Batch Processes Using State Equipment Networks. AIChE J. 58, 3416–3432. doi:10.1002/aic

Nie, Y., Biegler, L.T., Villa, C.M., Wassick, J.M., 2015. Discrete time formulation for the integration of scheduling and dynamic optimization. Ind. Eng. Chem. Res. 54, 4303–4315. doi:10.1021/ie502960p

Patil, B.P., Maia, E., Ricardez-Sandoval, L., 2015. Integration of Scheduling, Design, and Control of Multiproduct Chemical Processes Under Uncertainty. AIChE J. 61, 2456–2470. doi:10.1002/aic

Pistikopoulos, E.N., Diangelakis, N.A., 2015. Towards the integration of process design, control and scheduling: Are we getting closer? Comput. Chem. Eng. 91, 85–92. doi:10.1016/j.compchemeng.2015.11.002

Pistikopoulos, E.N., Diangelakis, N.A., Oberdieck, R., Papathanasiou, M.M., Nascu, I., Sun, M., 2015. PAROC—An integrated framework and software platform for the optimisation and advanced model-based control of process systems. Chem. Eng. Sci. 136, 115–138. doi:http://dx.doi.org/10.1016/j.ces.2015.02.030

Rafiei-Shishavan, M., Mehta, S., Ricardez-Sandoval, L.A., 2017a. Simultaneous design and control under uncertainty: A back-off approach using power series expansions. Comput. Chem. Eng. 99, 66–81. doi:10.1016/j.compchemeng.2016.12.015

Rafiei-Shishavan, M., Ricardez-Sandoval, L.A., 2017b. A Stochastic Approach for Integration of Design and Control under Uncertainty: A Back-off Approach Using Power Series Expansions, in: Espuña, A., Graells, M., Puigjaner, L. (Eds.), 27th European Annual Symposium on Computer Aided Chemical Engineering. Elsevier, pp. 1861–1866. doi:http://dx.doi.org/10.1016/B978-0-444-63965-3.50312-3

Ricardez Sandoval, L.A., Budman, H.M., Douglas, P.L., 2008. Simultaneous design and control of processes under uncertainty: A robust modelling approach. J. Process Control 18, 735–752. doi:10.1016/j.jprocont.2007.11.006

Ricardez-Sandoval, L.A., 2012. Optimal design and control of dynamic systems under uncertainty: A probabilistic approach. Comput. Chem. Eng. 43, 91–107. doi:10.1016/j.compchemeng.2012.03.015

Ricardez-Sandoval, L.A., Budman, H.M., Douglas, P.L., 2009. Integration of design and control for chemical processes: A review of the literature and some recent results. Annu. Rev. Control 33, 158–171. doi:10.1016/j.arcontrol.2009.06.001

Sakizlis, V., Perkins, J.D., Pistikopoulos, E.N., 2004. Recent advances in optimization-based simultaneous process and control design. Comput. Chem. Eng. 28, 2069–2086. doi:10.1016/j.compchemeng.2004.03.018

Sanchez-Sanchez, K., Ricardez-Sandoval, L., 2013. Simultaneous Process Synthesis and Control Design under Uncertainty: A Worst-Case Performance Approach. AIChE J. 59, 2497–2514. doi:10.1002/aic

Seferlis, P., Georgiadis, M.C., 2004. The Integration of Process Design and Control, Computer-Aided Chemical Engineering. Elsevier Ltd.

Sharifzadeh, M., 2013. Integration of process design and control: A review, Chemical Engineering Research and Design. Institution of Chemical Engineers. doi:10.1016/j.cherd.2013.05.007

Shi, J., Biegler, L.T., Hamdan, I., Wassick, J.M., 2016. Optimization of grade transitions in polyethylene solution polymerization processes. Comput. Chem. Eng. 62, 1126–1142. doi:10.1002/aic.15113

Srinivasan, B., Bonvin, D., Visser, E., Palanki, S., 2002. Dynamic optimization of batch processes II. Role of measurements in handling uncertainty. Comput. Chem. Eng. 27, 27–44.

Terrazas-Moreno, S. and, Flores-Tlacuahuac, A., Grossmann, I.E., 2008. Simultaneous Design, Scheduling, and Optimal Control of a Methyl-Methacrylate Continuous Polymerization Reactor. AIChE J. 54, 3160–3170. doi:10.1002/aic

Trainor, M., Giannakeas, V., Kiss, C., Ricardez-Sandoval, L.A., 2013. Optimal process and control design under uncertainty: A methodology with robust feasibility and stability analyses. Chem. Eng. Sci. 104, 1065–1080. doi:10.1016/j.ces.2013.10.017

Vega, P., Lamanna de Rocco, R., Revollar, S., Francisco, M., 2014. Integrated design and control of chemical processes – Part I: Revision and classification. Comput. Chem. Eng. 71, 602–617. doi:10.1016/j.compchemeng.2014.05.010

Yuan, Z., Chen, B., Sin, G., Gani, R., 2012. State-of-the-Art and Progress in the Optimization-based Simultaneous Design and Control for Chemical Processes. AIChE J. 58, 1640–1659. doi:10.1002/aic

Zhuge, J., Ierapetritou, M.G., 2016. A Decomposition Approach for the Solution of Scheduling Including Process Dynamics of Continuous Processes. Ind. Eng. Chem. Res. 55, 1266–1280. doi:10.1021/acs.iecr.5b01916

Zhuge, J., Ierapetritou, M.G., 2012. Integration of scheduling and control with closed loop implementation. Ind. Eng. Chem. Res. 51, 8550–8565. doi:10.1021/ie3002364

Appendices

Appendix A: Orthogonal Collocation on Finite Elements

In orthogonal collocation on finite elements, each finite element is divided into a number of collocation points. In this work, the number of collocation points is 5. One benefit of orthogonal collocation is that the derivative $\dot{\boldsymbol{x}}$ can be estimated from the values $\boldsymbol{x}$ at each collocation point, as shown in (A.1). The matrix entries $\mathcal{A}_{k,k'}$ defines the weighting that each point k' has towards the derivative at point k, and is defined in (A.2) using the Lagrange polynomial $\ell_{k'}(r_k)$ in (A.3), where the roots $\boldsymbol{r}$ are analogous to dimensionless time within each finite element, and are defined as the roots of the Legendre polynomial which lie within [0,1]. For finite elements of non-unit lengths, the derivative must be scaled using δt_i, as in (A.1).

$$\dot{\boldsymbol{x}}_{ijk} = \frac{\sum_{k'} \mathcal{A}_{kk'} \boldsymbol{x}_{ijk'}}{\delta t_i} \quad \forall\, i,j,k \tag{A.1}$$

$$\mathcal{A}_{kk'} = \frac{\partial \ell_{k'}(r_k)}{\partial r} \quad \forall\, k,k' \tag{A.2}$$

$$\ell_{k'}(r_k) = \prod_{\substack{k''=1,\\ k''\neq k'}}^{K} \frac{r_k - r_{k''}}{r_{k'} - r_{k''}} \quad \forall\, k,k' \tag{A.3}$$

The model in the CSTR case study is discretized into indices i,j,k. The number of regions I is required to be 10, in order to be double the number of product grades, which is 5. The number of finite elements J is selected to be 100 to allow for long production times of one hour, and to provide a reasonable balance between speed and accuracy. The number of collocation points K is selected to be 5 to allow for a fourth-order polynomial approximation. To ensure zero- and first-order continuity of $\boldsymbol{x}_{CSTR}$, for $\boldsymbol{x}_{CSTR} = \{T, C_B\}$, (A.4) through (A.15) must be included in the problem formulation for the CSTR case study. These equations are analogous to the general form shown in Section 3.3 as Eq. (4)-(7), except here they are shown expanded and in discrete form, exactly as they are implemented.

$$C_{B_{i,j,5}} = C_{B_{i,j+1,1}} \quad \forall i,j \tag{A.5}$$

$$C_{B_{i,100,5}} = C_{B_{i+1,1,1}} \quad \forall i \tag{A.6}$$

$$\frac{\sum_{k'} \mathcal{A}_{5,k'} C_{B_{i,j,k'}}}{\delta t_i} = \frac{\sum_{k'} \mathcal{A}_{1,k'} C_{B_{i,j+1,k'}}}{\delta t_i} \quad \forall i,j \tag{A.7}$$

$$\frac{\sum_{k'} \mathcal{A}_{5,k'} C_{B\,i,100,k'}}{\delta t_i} = \frac{\sum_{k'} \mathcal{A}_{1,k'} C_{B\,i+1,1,k'}}{\delta t_{i+1}} \quad \forall i \tag{A.8}$$

$$T_{i,j,5} = T_{i,j+1,1} \quad \forall i,j \tag{A.9}$$

$$T_{i,100,5} = T_{i+1,1,1} \quad \forall i \tag{A.10}$$

$$\frac{\sum_{k'} \mathcal{A}_{5,k'} T_{i,j,k'}}{\delta t_i} = \frac{\sum_{k'} \mathcal{A}_{1,k'} T_{i,j+1,k'}}{\delta t_i} \quad \forall i,j \tag{A.11}$$

$$\frac{\sum_{k'} \mathcal{A}_{5,k'} T_{i,100,k'}}{\delta t_i} = \frac{\sum_{k'} \mathcal{A}_{1,k'} T_{i+1,1,k'}}{\delta t_{i+1}} \quad \forall i \tag{A.12}$$

Appendix B. Set-point Determination from Binary Sequence Matrix

In the problem formulations, the function $\boldsymbol{\psi}_{ijk}$ maps the binary sequencing matrix $\boldsymbol{\mathcal{S}}$ to a profile of set-points $\boldsymbol{y}_{ijk}^{sp}$ $\forall\, i,j,k$. Within the binary matrix $\boldsymbol{\mathcal{S}}$, element $\mathcal{S}_{g,g'}$ indicates if set-point $\mathrm{Y}_{g'}^{sp}$ is being produced g^{th} in the sequence. Note that the index of grades g is a subset of the index of time regions i, so some values of i may be used as the index for $\mathcal{S}_{g,g'}$ or β_g, in place of g. The list of set-points $\mathbf{Y}^{\mathrm{sp}}$ is known *a priori*. Linear transitions between set-points are applied during transition regions (odd-numbered regions). As mentioned in Appendix A, $\boldsymbol{r}$ represent the roots of the Legendre polynomial which lie within [0,1].

$$\boldsymbol{\psi}_{ijk}(\boldsymbol{\mathcal{S}}) = \begin{Bmatrix} \beta_G + (\beta_1 - \beta_G)(j - 1 + r_k) & for\ i = 1 \\ \beta_{i/2} & for\ i = 2,4,6, \ldots I \\ \beta_{\frac{i-1}{2}} + \left(\beta_{\frac{i+1}{2}} - \beta_{\frac{i-1}{2}}\right)(j - 1 + r_k) & for\ i = 3,5,7, \ldots (I-1) \end{Bmatrix} \forall\, j,k \tag{B.1}$$

$$where\ \beta_g = \sum_{g'} \mathcal{S}_{g,g'}\, \mathrm{Y}_{g'}^{sp} \quad \forall g$$